TTI-2-8-75-207-6

TEXAS
TRANSPORTATION
INSTITUTE

STATE DEPARTMENT
OF HIGHWAYS AND
PUBLIC TRANSPORTATION

COOPERATIVE
RESEARCH

RESIDUAL STRESSES DUE TO TRAVELING LOADS AND REFLECTION CRACKING

in cooperation with the
Department of Transportation
Federal Highway Administration

RESEARCH REPORT 207-6

STUDY 2-8-75-207

FLEXIBLE PAVEMENT EVALUATION

TECHNICAL REPORT STANDARD TITLE PAGE

1. Report No.	2. Government Accession No.	3. Recipient's Catalog No.
FHWA/TX-79/18+207-6		

4. Title and Subtitle	5. Report Date
RESIDUAL STRESSES DUE TO TRAVELING LOADS AND REFLECTION CRACKING	June, 1979
	6. Performing Organization Code
7. Author(s)	8. Performing Organization Report No.
W. O. Yandell and R. L. Lytton	Research Report 207-6
9. Performing Organization Name and Address Texas Transportation Institute Texas A&M University College Station, Texas 77843	10. Work Unit No.
	11. Contract or Grant No. Study 2-8-75-207
	13. Type of Report and Period Covered Interim - September, 1974 June, 1979
12. Sponsoring Agency Name and Address Texas State Department of Highways and Public Transportation Transportation Planning Division P. O. Box 5051; Austin, Texas 78763	14. Sponsoring Agency Code

15. Supplementary Notes

Work done in cooperation with FHWA, DOT.
Study Title: Flexible Pavement Evaluation and Rehabilitation

16. Abstract

This report demonstrates some of the potential capabilities of the three dimensional mechano-lattice stress-strain analysis for predicting rut depth, fatigue cracking, corrugations and reflection cracking. The mechano-lattice analogy is the only technique available which is capable of predicting the behavior of linear or non-linear elasto-plastic or energy absorbing material subjected to directional traveling wheel loads. It is a rigorous technique that preserves equilibrium and has strain compatibility.

The problems investigated in this report are: the repeated one directional pneumatic tire rolling on a single layer of a compacted elasto-plastic sand-clay-water mixture with various boundary conditions and the behavior of an elasto-plastic overlay with potential reflection cracking. The build-up of residual stresses and strains is demonstrated to have significant effects on the accuracy of present day pavement design and construction procedures including rutting and fatigue crack prediction.

17. Key Words	18. Distribution Statement
Residual stresses and strains, traveling loads, reflection cracking, flexible pavement.	No Restrictions. This document is available to the public through the National Technical Information Service, Springfield, Virginia 22161

19. Security Classif. (of this report)	20. Security Classif. (of this page)	21. No. of Pages	22. Price
Unclassified	Unclassified	88	

Form DOT F 1700.7 (8-69)

RESIDUAL STRESSES DUE TO TRAVELING LOADS AND REFLECTION CRACKING

by

W. O. Yandell and R. L. Lytton

Research Report Number 207-6

Flexible Pavement Evaluation and Rehabilitation

Research Study 2-8-75-207

conducted for

The Texas State Department of Highways and
Public Transportation

in cooperation with the
U. S. Department of Transportation
Federal Highway Administration

by the

Texas Transportation Institute
Texas A&M University
College Station, Texas

June 1979

ABSTRACT

This report demonstrates some of the potential capabilites of the three dimensional mechano-lattice stress-strain analysis for predicting rut depth, fatigue cracking, corrugations and reflection cracking. The mechano-lattice analogy is the only technique available which is capable of predicting the behavior of linear or non-linear elasto-plastic or energy absorbing material of any stiffness subjected to directional traveling wheel loads. It is a rigorous technique that preserves equilibrium and has strain compatibility.

The problems investigated in this report are: the repeated one directional pneumatic tire rolling on a single layer of a compacted elasto-plastic material with various boundary conditions and the behavior of an elasto-plastic overlay with potential reflection cracking. The build-up of residual stresses and strains is demonstrated to have significant effects on the accuracy of present day pavement design and construction procedures including rutting and fatigue crack prediction.

SUMMARY

This report presents the results of a three dimensional stress-strain analysis called the mechano-lattice analogy. The technique is used here to simulate the stress-strain behavior of a single layered elasto-plastic pavement subjected to repeated rolling in one direction by a pneumatic tire. The mechano-lattice analysis is the only presently known way of analyzing such a problem realistically and quantitatively. It is able to simulate any non-linear, energy absorbing or plastic behavior or Poisson's Ratio of a material using a rigorous technique that preserves equilibrium and has strain compatibility.

The calculated results showed that when material parameters remain constant, rutting and longitudinal material flow and build-up of residual stresses continue at an accelerating rate as wheel passes continue. The knowledge of this behavior is useful in explaining the mechanism of corrugation formation, the rate at which critical tensile regions in the pavement are reduced by accumulated residual stresses and the slow down of rutting rate due to the increasing strength of the materials. This increase of strength can be inferred from calculated residual mean stress and from calculated increasing density of the material.

The analysis was also used for investigating the stress-strain behavior in an overlay over an opening and closing crack in an underlying old pavement. The analysis was able to predict some of the behavior of a laboratory test simulating the same problem. The analysis predicted that the overlay material will continually move toward the crack and form a hump which would be further modified by traffic. The high tensile stresses caused by the

crack opening would tend to be reduced by residual stresses built up in the overlay by passing traffic.

The mechano-lattice analysis will have many uses in pavement design, construction and maintenance.

1. When applied to multilayer pavements it will be used for predicting shift factors in the number of repetitions to failure in laboratory tests of fatigue cracking and rutting, to the actual number of repetitions observed in the field. More broadly, it can be used for investigating the validity of failure mechanisms on which current design methods are based.

2. It can be used for calculating the number of roller passes to achieve a desired level of compaction.

3. It could be used in the investigation of the cause and the critical material properties involved in maintenance problems such as corrugations and roughness.

4. The technique can also be used for the investigation of the cause and remedy of reflection cracking.

IMPLEMENTATION STATEMENT

Even with the best analysis tools that have been developed up to the present time, including linear elastic and viscoelastic theory, it has been impossible to predict the field behavior of pavements in fatigue, rutting, and reflection cracking directly from the properties of pavement materials as they are measured in the lab. This report documents the development of a new such tool that shows promise of being able to predict fatigue life, rutting behavior, and even reflection cracking directly from the laboratory-measured material properties. Many figures are shown of the calculated results to give a good feel for the physical effects that occur in a pavement which accumulates stresses and strains under traveling wheel loads. The analysis is applicable to all flexible pavement materials since they are all elasto plastic to some degree.

Results of calculations with this computer program will serve as a reference for decision making concerning the improvement of pavement design techniques, particularly for fatigue cracking, rutting, and reflection cracking.

TABLE OF CONTENTS

List of Figures

INTRODUCTION

The problems of reflection cracking, rutting, and fatigue of flexible pavements have been the subject of numerous analyses and research studies because of their importance to the pavement maintenance and rehabilitation budgets of highway agencies. There has always been a conviction that if the stresses and strains that develop in a pavement under load could be understood and predicted, then better and more economical pavements could be designed and built. All of these studies have attempted to represent the actual stress-strain behavior of the pavement materials for it has been known that a proper characterization of the material properties was essential to a proper understanding and reliable prediction of pavement behavior. The use of linear elastic and linear viscoelastic theory have been the most recent attempts to predict distress in pavements.

In no case up to the present time have there been any attempts to investigate the effect of plastic hysteresis in pavement materials. The fact that asphaltic concrete materials follow different stress-strain paths on loading and unloading has been known for many years but the incorporation of that knowledge into the prediction of pavement behavior has been neglected. The reason for this neglect is obvious: heretofore, the use of hysteresis properties in pavement analysis was regarded as too formidable a task to attempt or too expensive of computer time.

To the knowledge of the authors of this report, this represents the first attempt to investigate the effects of hysteresis, residual stresses, and residual strains on the actual behavior of pavement materials under load. The analysis method is unique since it allows for the representation

of the effects of a traveling load (fatigue and rutting) and an opening and closing crack in an underlying pavement (reflection cracking). The results of the analysis are presented in numerous figures so that a proper appreciation may be gained not only of the power of the analytical tool but also of the physical effects that are predicted.

In the past, the theory of linearized elasticity has been useful in assisting with pavement design. For example, the Shell method uses the elastic strain magnitude at the base of layers together with laboratory fatigue life. If the pavement can become progressively unservicable with time it is clearly not a elastic structure. Hence a more realistic approach than that afforded by linear elastic analysis is needed if the theoretical prediction of the many forms of pavement distress are to be accurate. Types of elasto-plastic and visco-elastic finite element analyses are able to predict the deformation for stationary repeated loading but are not able to simulate the stress-strain behavior experienced by a road pavement when traveling, rather than pulsing loads, operate. A recent exception is the work of Battiato et al. (1) where a two layered system was considered to be viscoelastic and incompressible. Only qualitative deformational information results.

The mechano-lattice analogy was devised (2) (3) in 1967 to provide a stress-strain analysis for real materials. Non-linear energy absorbing elastic and elasto-plastic materials can be simulated with any Poisson's Ratio. This has been done for rubber sliding triaxially with gross deformation (4) and for repeated rolling of an elasto-plastic road pavement which was found to build up longitudinal residual stresses with each one directional pass. The road material was shown to flow in the opposite direction to that of

rolling.

The present study investigates the behavior of an elasto-plastic pavement or overlay subjected to repeated by a pneumatic tire traveling in one direction along a fixed wheel path. A plane strain analysis of an elasto-plastic overlay stressed by an opening and closing crack in the underlying pavement is also studied.

The Mechano-Lattice Stress-Strain Analysis

The two and three dimensional mechano-lattice analogy was originally developed (2) to provide a means of determining the stress-strain behavior of all linear and non-linear elastic materials as well as those that exhibit plastic and or energy absorbing behavior. A more complex version (5), (6), that can handle gross deformation has been used successfully in many predictions of hysteretic friction in polymers (7), (8). The technique preserves equilibrium, has strain compatibility and can handle geometric and material non-linearity.

Road materials have various degrees of non-linearity, damping, and plasticity; more so when they are constituents of roads that are either slowly or quickly becoming unserviceable. The present investigation studies a section of elasto-plastic pavement in three dimensions. An elasto-plastic material is assumed here to be one which when loaded, deflects, and when the load is removed a permanent but smaller deflection remains. The behavior of the material in the investigation is simplified. Figure 1 shows how a measured load-unload cycle on a load-deflection plot is simplified by two straight lines, one for loading, the other for unloading. Such simplification is not necessary for a solution but speeds it.

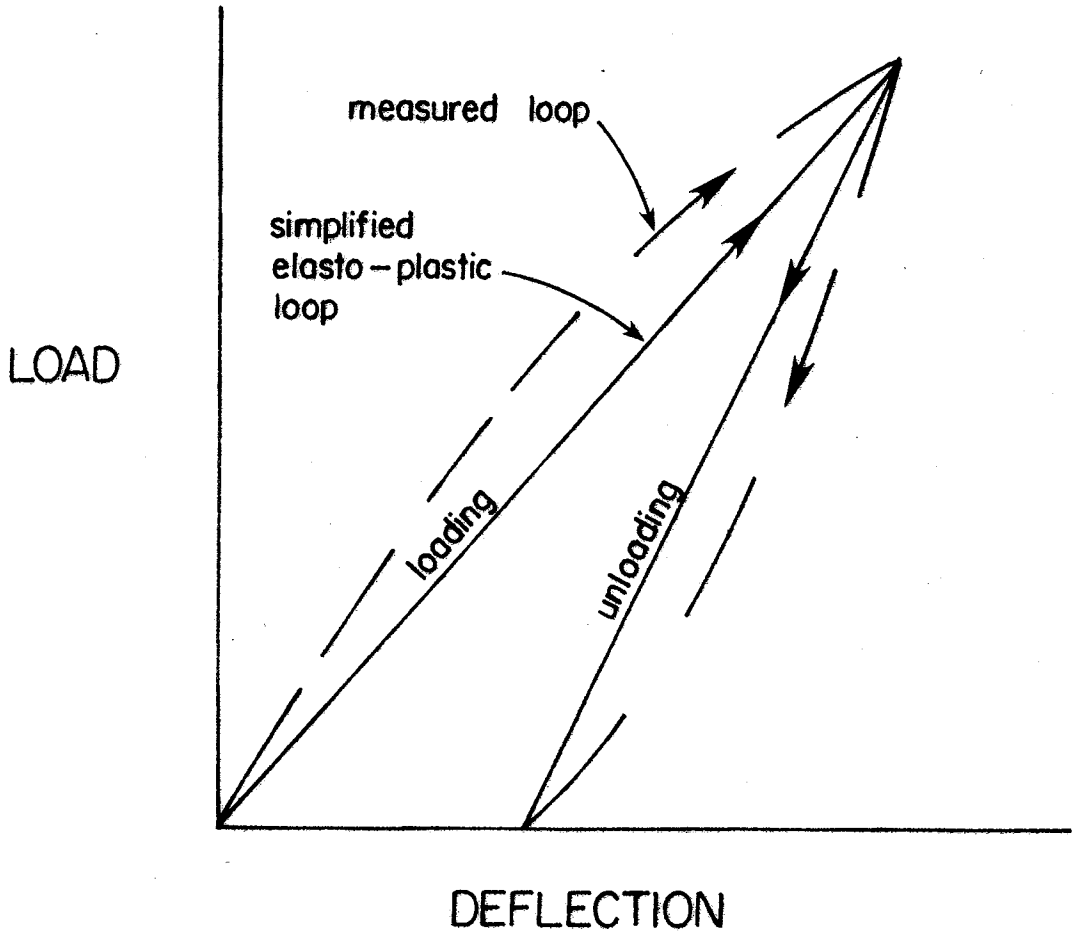

Figure 1. Simplification of elasto-plastic hysteresis loop.

The behavior exhibited by Figure 1 is incorporated in each element of a unit of the mechano-lattice analogy (Fig. 2). Each element has one compliance for loading and another compliance for unloading. The shear and the volume deflection behavior are separated to allow any Poisson's Ratio to be simulated. If for example one of these units is subjected to a reversing load unconfined compression-tension test, the load deflection path could be that shown in Figure 3. The stiffness factors of all 28 elements are calculated so that the stress-strain behavior is identical to that of the material being simulated. The stresses at the center of a unit are the resolution of the forces in the elements belonging to the unit divided by the area of a unit's side.

To simulate one side of the laterally symmetric elasto-plastic pavement for the repeated rolling problem, 840 of the above units are connected at their eight corners by frictionless joints (Fig. 4). The load of a pneumatic tire is represented by downward vertical loads applied to some of the top surface joints. The numerical solution is obtained by calculating forces in the elements taking load history into account. The load history depends on the direction of rolling. The element forces and outside loads on joints are resolved vertically, longitudinally, and laterally. The joints are then moved in the direction of the forces in an overdamped way. This process is repeated until all the joints are in equilibrium. The stresses can then be calculated.

The Repeated Rolling Problem

The major part of the investigation consists of a simulated pneumatic tire with a surface of contact measuring one inch wide and two inches long

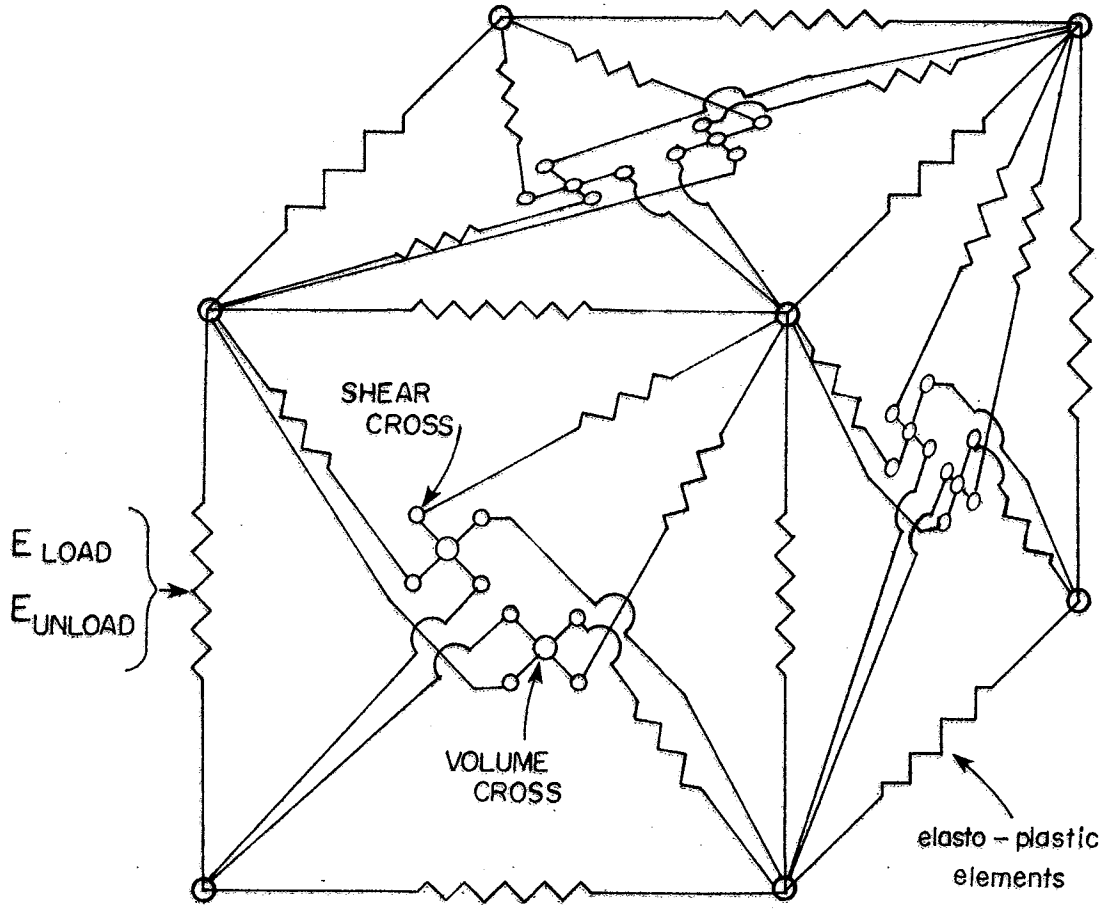

APPROXIMATE ANALOGUE OF THREE DIMENSIONAL MECHANO – LATTICE UNIT

Figure 2. Mechanical counterpart of the three dimensional elasto-plastic simulation unit.

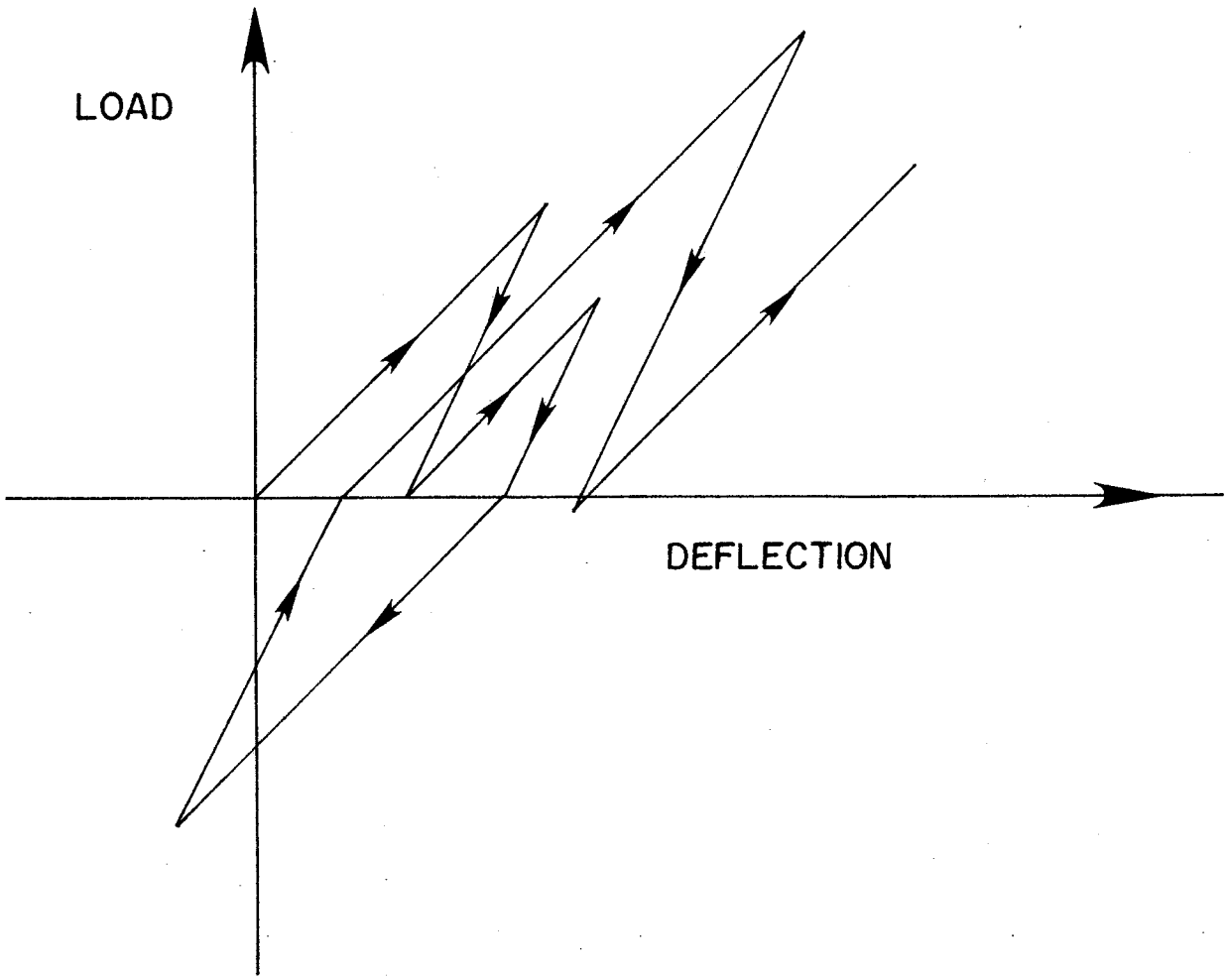

Figure 3. Possible load-deflection behavior of an element

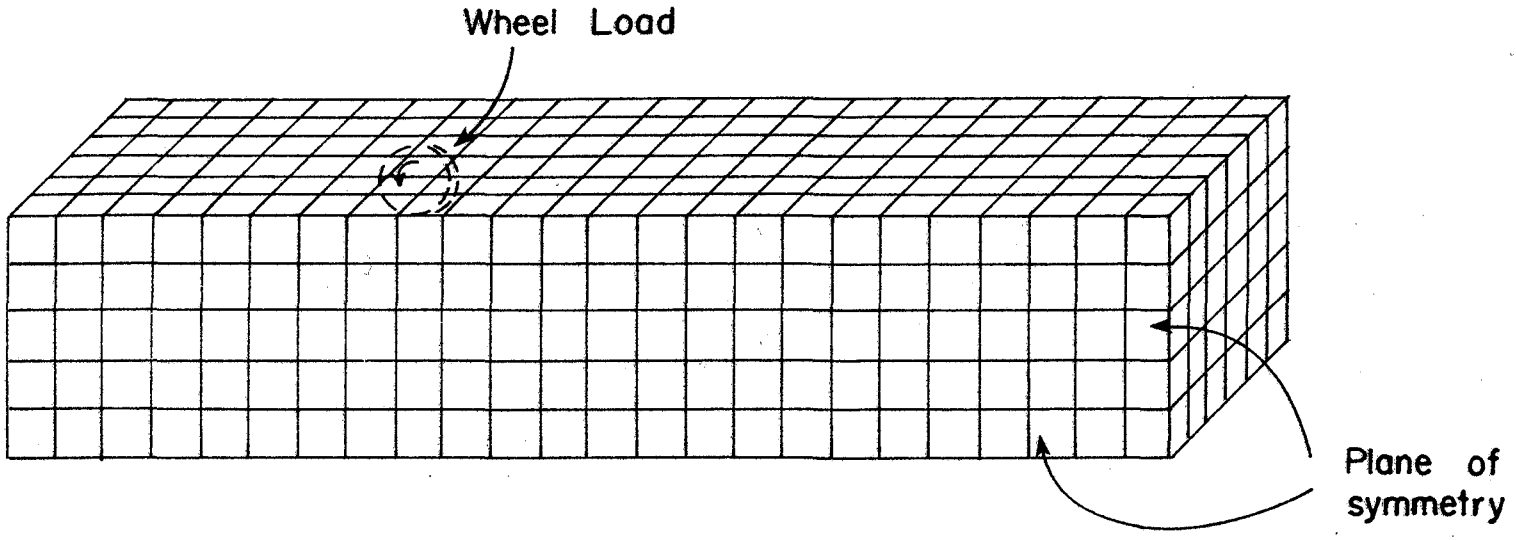

Figure 4. Assembly of elasto-plastic units to form one symmetric half of the simulated pavement.

rolling in one direction on a section of road material five inches deep, twelve inches wide and twenty four inches long. The sides and base of the material are restrained in all directions. The ends are allowed to move in such a way that homogeneous stress exists near the rear boundary. The residual stresses and strains resulting from the first pass remain in all of the material for the second pass and so on.

The pavement material is assumed to have the properties at the first cycle of load-unload of a mixture of 40% kaolinite, 60% graded sand, 12.4% moisture content and optimum Proctor density. The loading modulus is 5000 p.s.i. and the unloading modulus is 10,000 p.s.i. This gives 50% residual strains with load-unload in one direction. The Poisson's Ratio was 0.4. The following problems were solved:

(a) One through five passes of a 100-Pound load at 50 p.s.i. contact pressure and area of contact two square inches.

(b) One pass of a 200-Pound load with a contact pressure of 100 p.s.i. and area of contact two square inches.

(c) One pass of a 200-Pound load at a contact pressure of 50 p.s.i. and area of contact of four square inches.

(d) One pass of a 100-Pound load at a contact pressure of 50 p.s.i. and an area of contact of two square inches. In this case the sides of the simulated material were free to move in any direction.

The physical dimensions and material properties used in this illustrative problem are not significant to the phenomenological output of this mechano-lattice solution. The physical dimensions and material simulated were chosen to minimize computer time and because the material has been thoroughly testes by repeated loade tests on a volumetric and deformational basis. Similar tests need to be made on other pavement materials such as asphalt concrete, various base course materials, and so on. The analysis technique is needless to say applicable to all of them.

RESULTS OF ANALYSIS

Residual Strains

There are three types of cumulative strain associated with this study.

(a) Vertical residual strains constituting rutting due to the passage of the tire.

(b) Longitudinal residual strains that cumulate with each wheel pass to lead to longitudinal flow which varies in rate and direction across a cross section.

(c) Lateral residual strains that have indirect effects and will not be discussed here.

(a) Vertical Residual Strains

Figure 5 shows the deformed surface of the rut inverts for the first through the fifth wheel pass. The longitudinal sections show the transient profiles that move along with the wheel and the broken lines indicate the permanent rut inverts. As wheel passes continue, more of the rut deepening takes place further forward of the moving wheel. This is thought to be due to the build up of residual stresses. The enlarging deflection bowl also causes the rolling resistance to decrease from one in 833 to one in 1250 as the rut deepening for each pass increases. The rolling resistance is measured as the uphill grade of the surface of contact. The increase in rut deepening with load passes is shown in Figure 6.

The cross sections of the permanent rutting shows that the surface adjacent to the side of the rut sinks as the number of load passes increase. With the fifth pass, the material surface furthest from the wheel rises above the

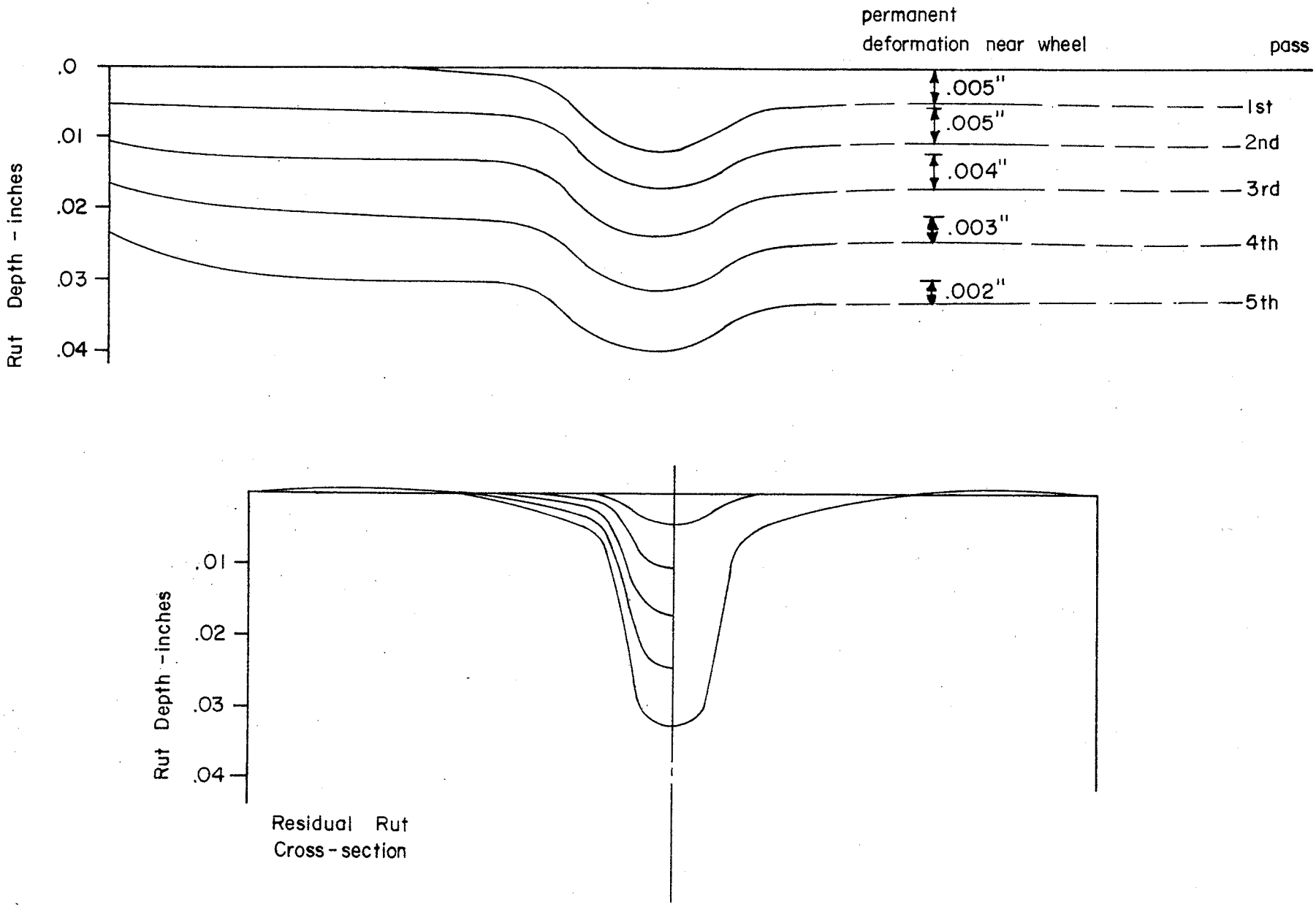

Figure 5. The variation in transient and permanent rut depth with number of wheel passes.

original surface. The table in Figure 6 also shows that the rebound of the rut invert also increases in rate per pass.

Doubling the load but holding pressure constant increases rut depth only slightly. Rolling resistance drops by 14%. Thus large contact areas are most desirable.

Doubling the load and also doubling contact pressure doubles rut deepening per pass. Rolling resistance also doubles.

Leaving the sides of the material unrestrained only slightly increases rut depth.

With the same set of load, contact area and material properties, rutting will continue at an increasing rate in spite of the continual build up of residual stresses. However an increase in residual mean stress will reduce the plastic component of the material properties and rutting will slow down or cease. When material properties vary spatially, rut depths will also vary causing more uneven riding.

(b) Longitudinal Residual Strains

As with the two dimensional analysis the material is moved permanently and unevenly in a longitudinal direction. Figure 7 shows the residual longitudinal movement distribution on a cross section after the first pass of a 100 lb loaded tire with a 50 p.s.i. vertical contact stress. The bulk of the material moves back in the opposite direction to that of travel. The material contacting the tire moves forward however. This forward movement per pass is accelerated with each pass. The fifth pass (Fig. 8) plotted to a scale one fifth as sensitive as the first pass shows that the bulk of the material has moved forward. This is the opposite effect to

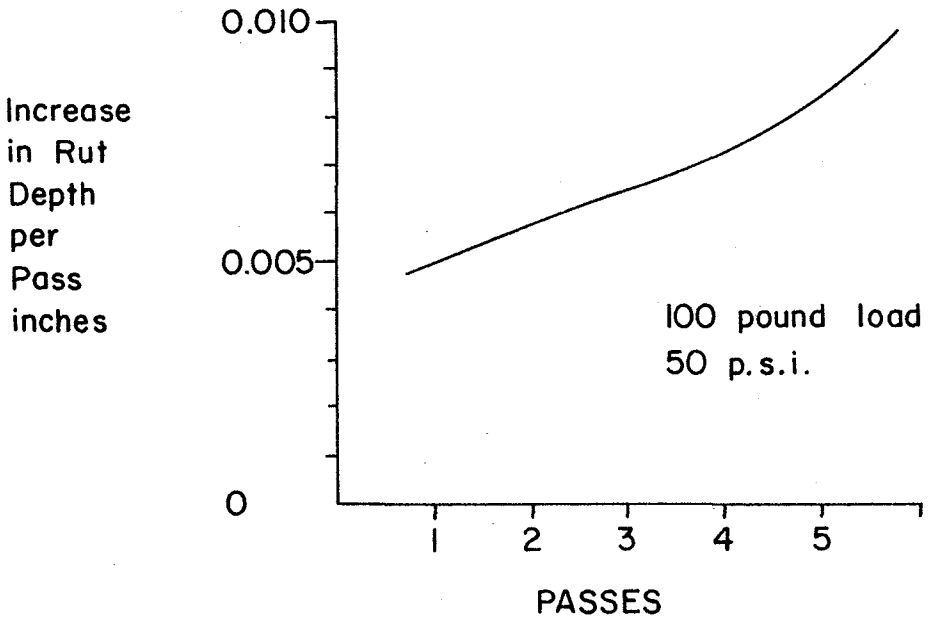

PASS	INCREASE IN RUT DEPTH FOR THIS PASS	RECOVERABLE RUT DEFLECTION FOR THIS PASS	ROLLING RESISTANCE
100 lb load at 50 p.s.i.			
1	0·00498 in	0·00613	1/833
2	0·00515 in	0·00627	
3	0·00639 in	0·00648	
4	0·00718 in	0·00677	
5	0·00833 in	0·00702	1/1250
100 lb load at 50 p.s.i. unrestrained at sides			
1	0·00508 in		1/833
200 lb load at 50 p.s.i.			
1	0·00567 in		1/710
200 lb load at 100 p.s.i.			
1	0·01005 in		1/416
5	0·01529 in		1/620

Figure 6. The increase in rut depth per wheel pass and as it varies with load and with contact pressure.

Figure 7. Residual longitudinal movement distribution after the first pass of a 100-pound load with a 50 p.s.i. contact pressure.

Scale: 0.1414 in = 0.00004 in defn

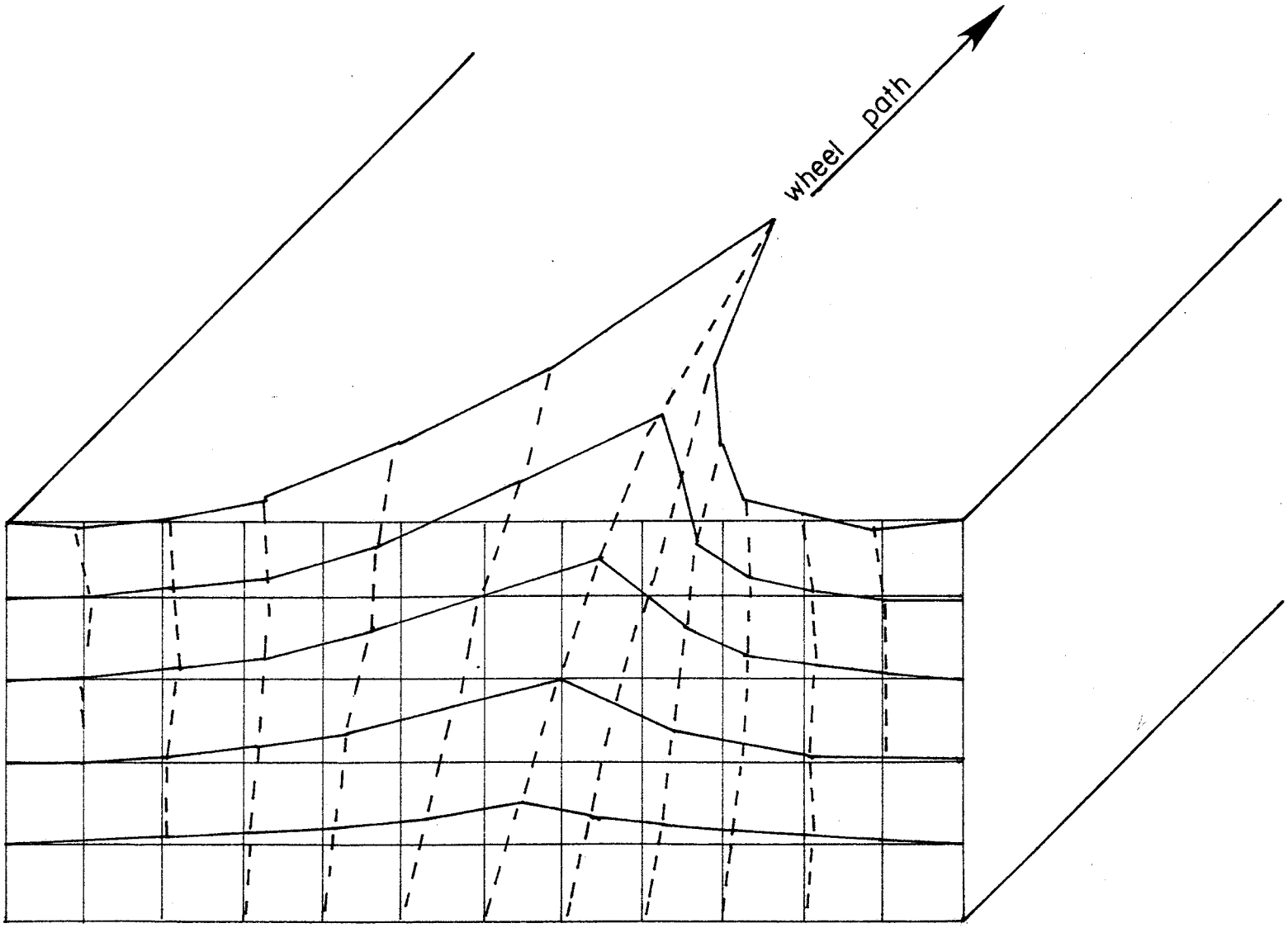

Figure 8. Residual longitudinal movement distribution after the fifth pass of a 100-pound load with a 50 p.s.i. contact pressure.

Scale: 0.1414 in = 0.0002 in defl^{n}

the similar analysis with plane stress (5) because in the present three dimensional analysis the sides are constrained and the material is levered forward by horizontal shear. This explanation is justified when Figure 7 is compared with Figure 9 which is a solution in which the sides were unrestricted. In this unrestricted case the material at the sides moves backward rather than the whole moving forward. The material contacting the tire however continues to move forward but at a reduced rate.

When the load and the contact pressure are doubled the longitudinal movement also doubles as seen by comparing Figure 10 with Figure 7. Doubling the load but keeping the contact stress constant also doubles the longitudinal movement and moves the deeper material more by proportion. See Figures 11 and 7. The same load applied over a larger area will cause more increases in longitudinal movement at depth.

Significance of Longitudinal Movement

The longitudinal movement associated with repeated rolling has at least two effects.

(a) The complex distribution of movement will cause the material to either gain strength by mastication or reduce it by increasing the effect of fatigue.

(b) As compaction due to traffic rolling continues, forward and backward longitudinal movement will also continue at a distribution and rate which are characteristics of the material. So when the material varies spatially the rate of longitudinal movement will vary spatially also, causing the buildup of bumps on the pavements.

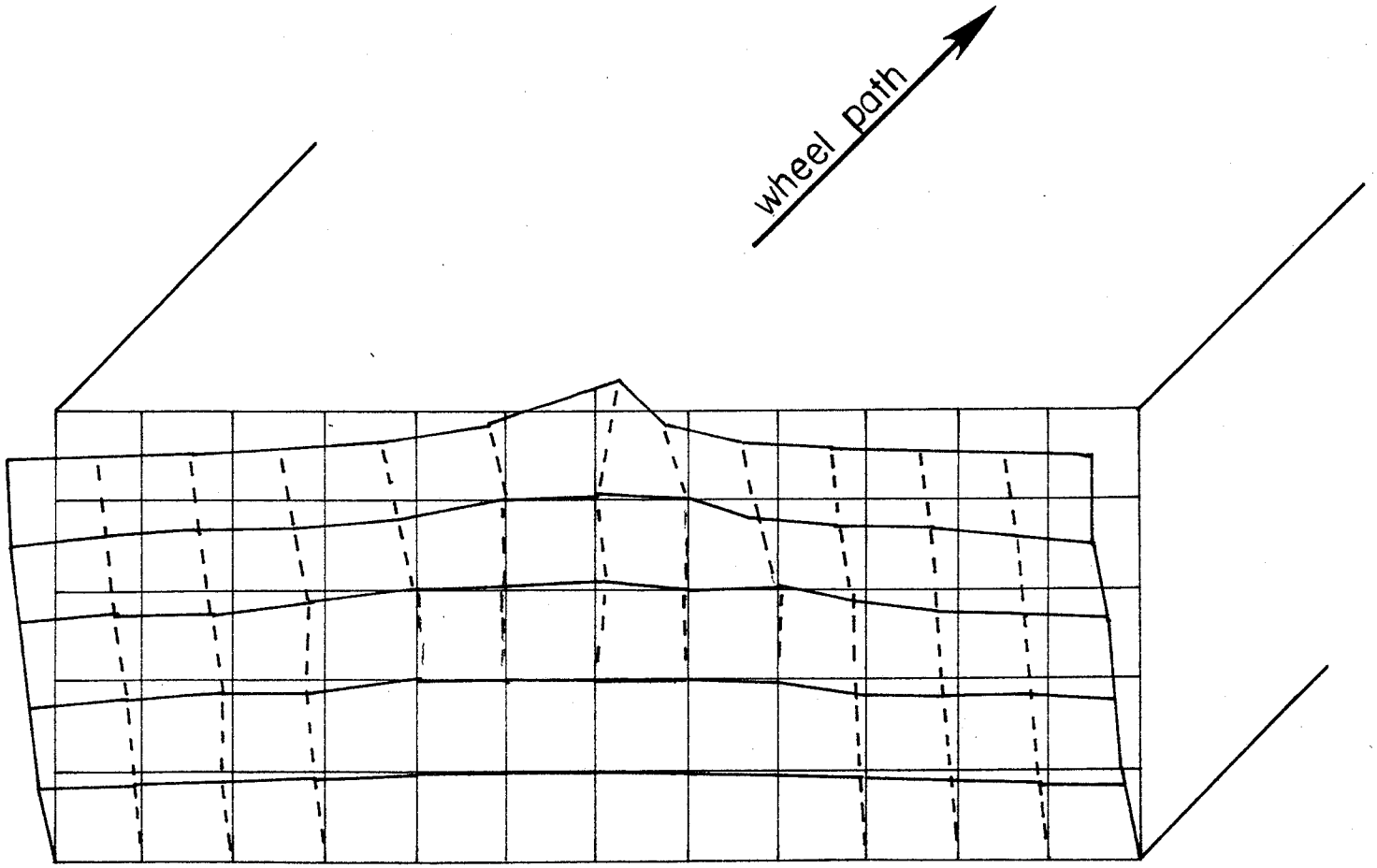

Figure 9. Residual longitudinal movement distribution after the first pass of a 100-pound load with a 50 p.s.i. contact pressure with no side restraint.

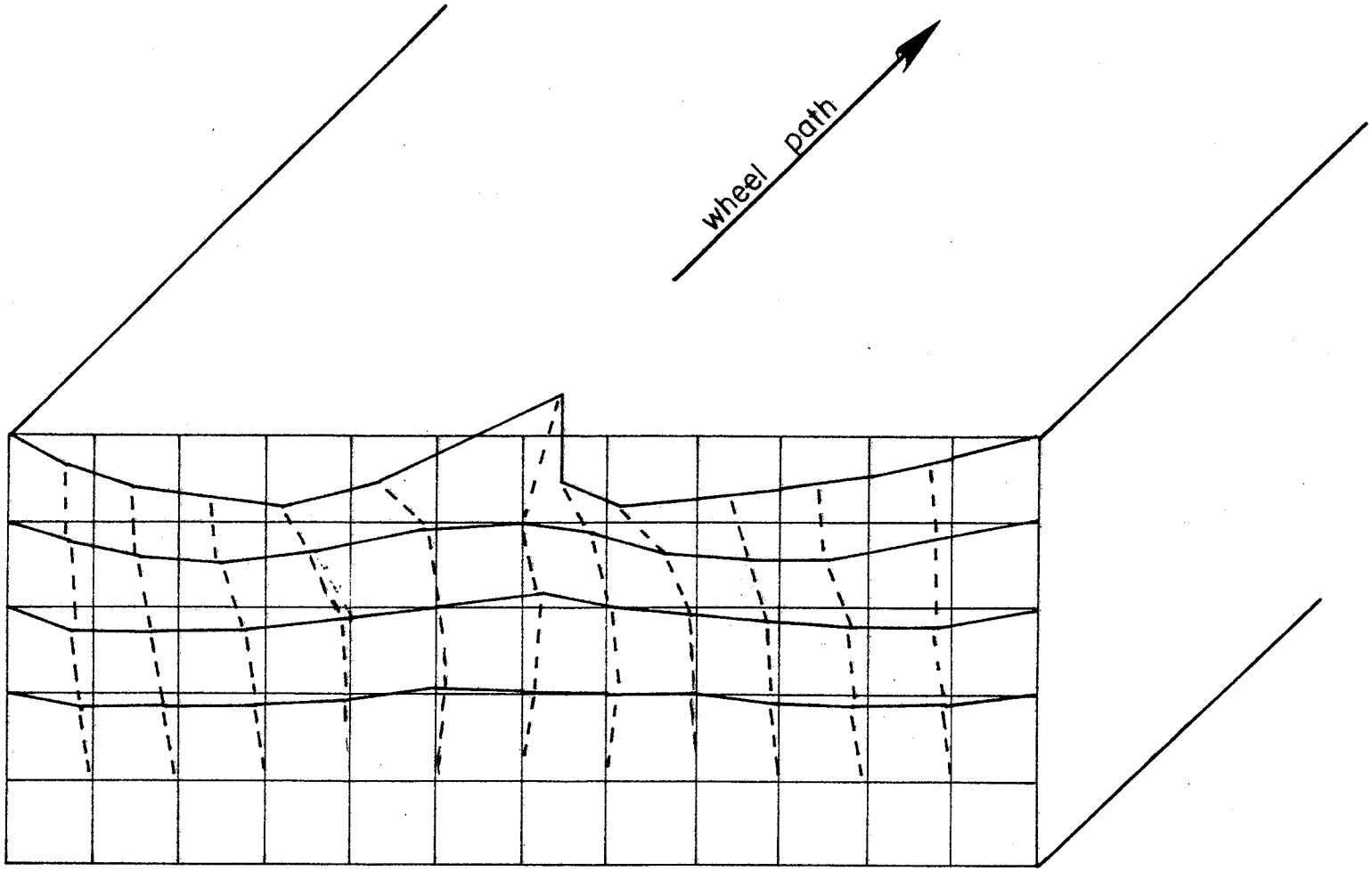

Figure 10. Residual longitudinal movement distribution after the first pass of a 200-pound load with a 100 p.s.i. contact pressure.

Scale: 0.1414 in = 0.00004 in defn

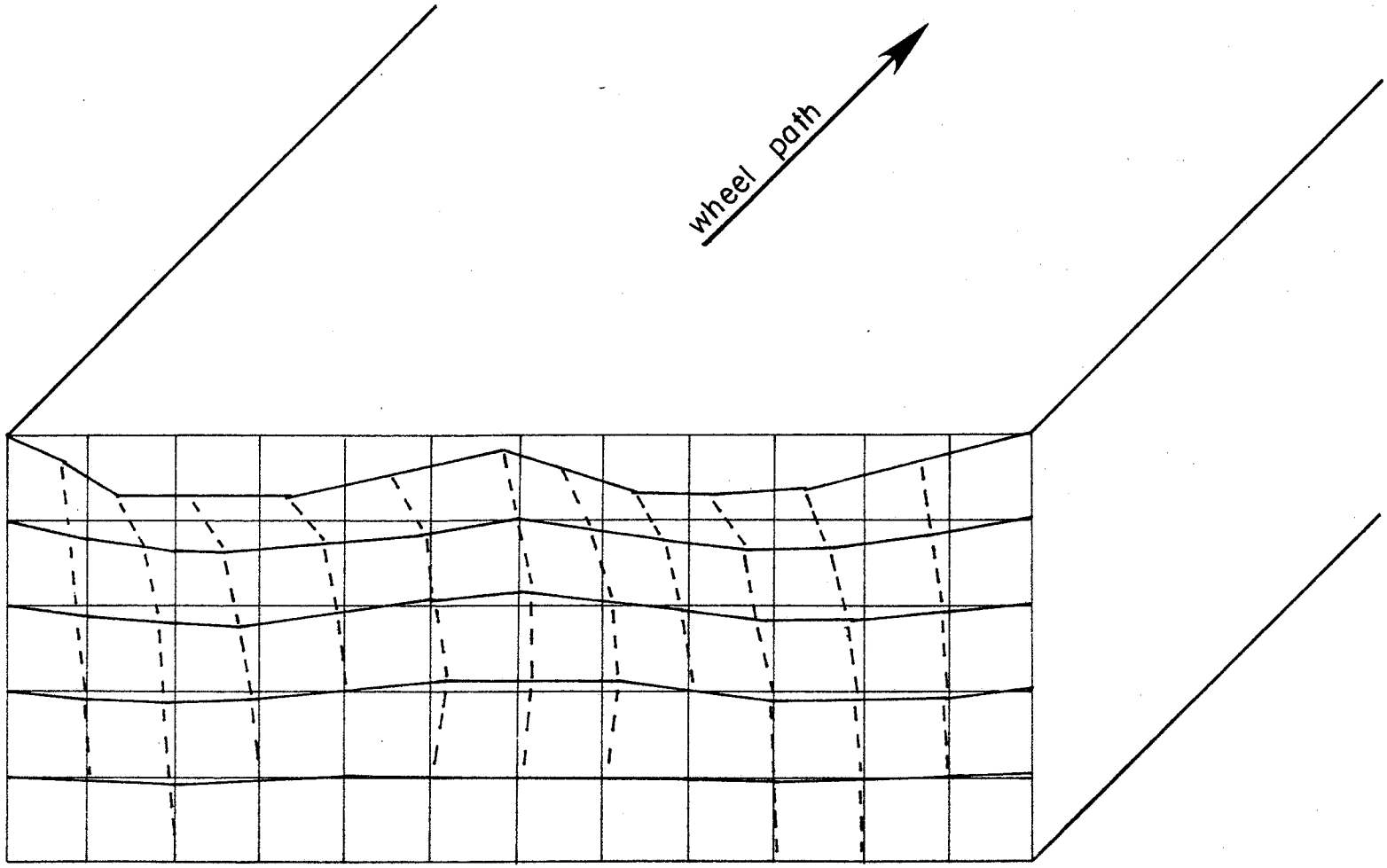

Figure 11. Residual longitudinal movement distribution after the first pass of a 200-pound load with a 50 p.s.i. contact pressure.

Scale: 0.1414 in = 0.00004 in defln

Stresses

Two types of stress are of interest in repeated rolling of elasto-plastic pavements-transient stresses that follow the rolling load and residual stresses that remain after the load has passed and which accumulate with each passing wheel.

(a) Residual Stresses in Unloaded Pavement

The analysis showed that with each pass the vertical (Figures 12 and 13) and the longitudinal residual stresses (Figures 14 and 15) build up rapidly directly under the wheel path when the 100 pound wheel at 50 p.s.i. is repeatedly passed. Lateral stresses (Figures 21 and 16) build to maxima below the surface and on either side of the wheel path after five passes. Figure 17 shows the increasing rate of build up.

When the load and contact stress are doubled to 200 pounds and 100 p.s.i. respectively all of the residual stresses (vertical, lateral, and longitudinal) are doubled on the first pass and form a similar set of patterns. This is seen by comparing Figure 12 with 18, 14 with 19, and 21 with 22. On the other hand when the load is doubled to 200 pounds but the contact stress is held constant at 50 p.s.i., by doubling the contact area, the increases in residual stresses over that for the 100 pound load are less. For instance the vertical residual stress increases by only 52% (Figure 12 and 23); the longitudinal residual stress increases by 80% (Figure 14 and 20) but the volume of material held in longitudinal compression is increased; the lateral residual stress still increases by 100% (Figures 21 and 24). These results indicate that the intensity of residual stress is increased

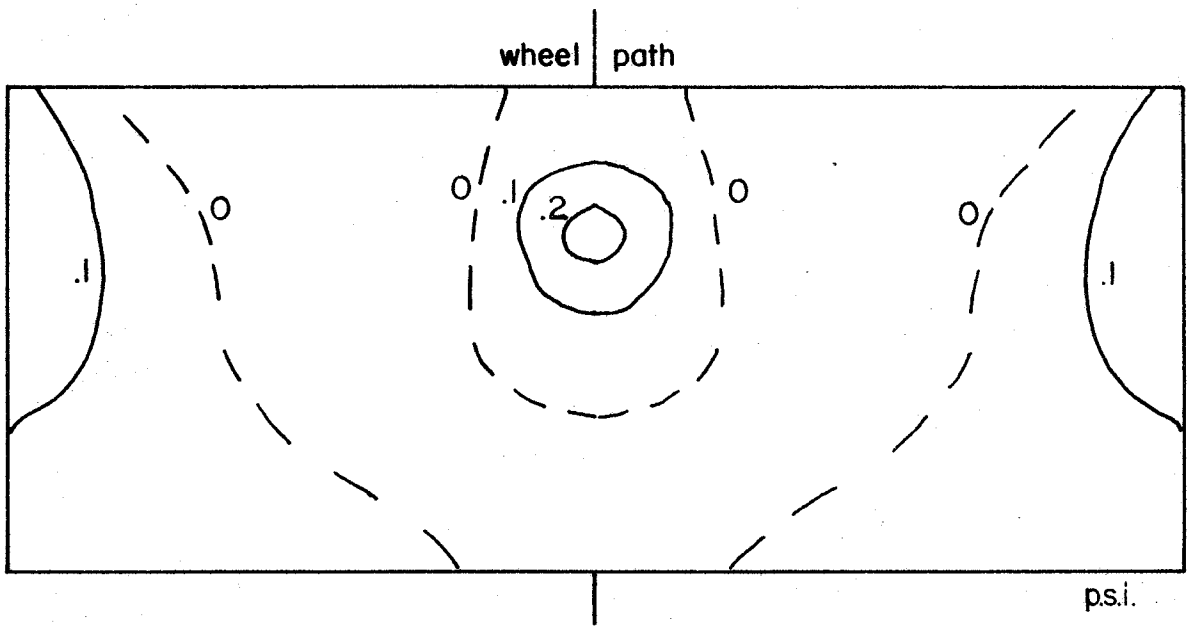

Figure 12. Cross-section of residual vertical stress distribution after the first pass of a 100-pound load with a 50 p.s.i. contact pressure.

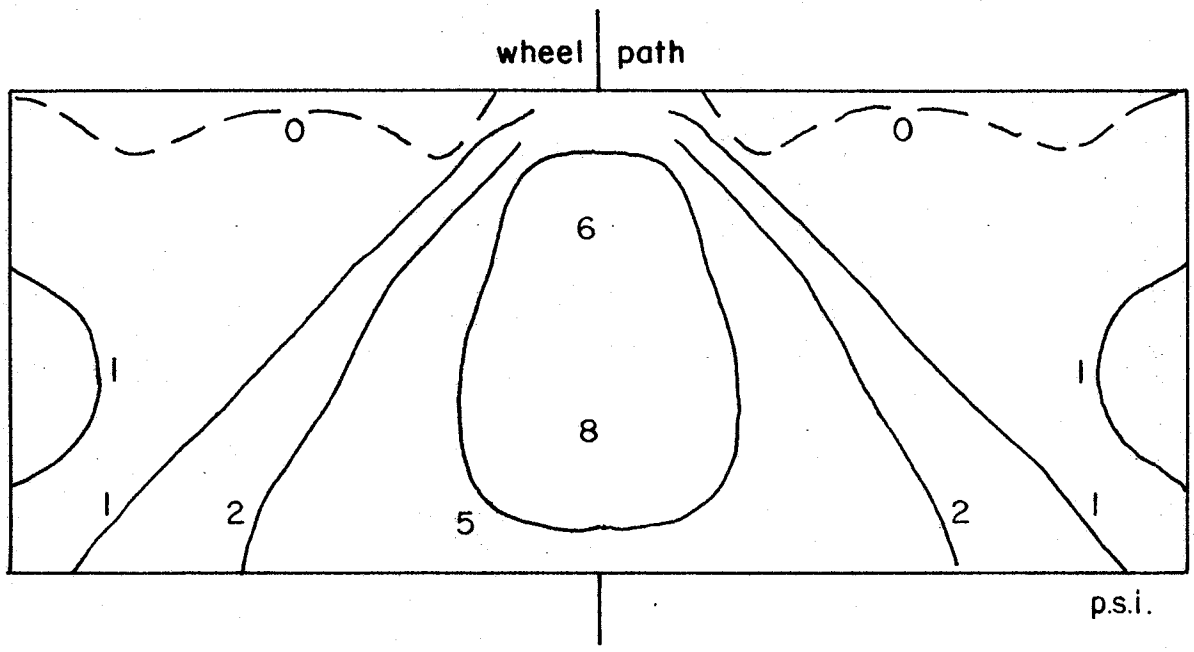

Figure 13. Cross-section of residual vertical stress distribution after the fifth pass of a 100-pound load with a 50 p.s.i. contact pressure.

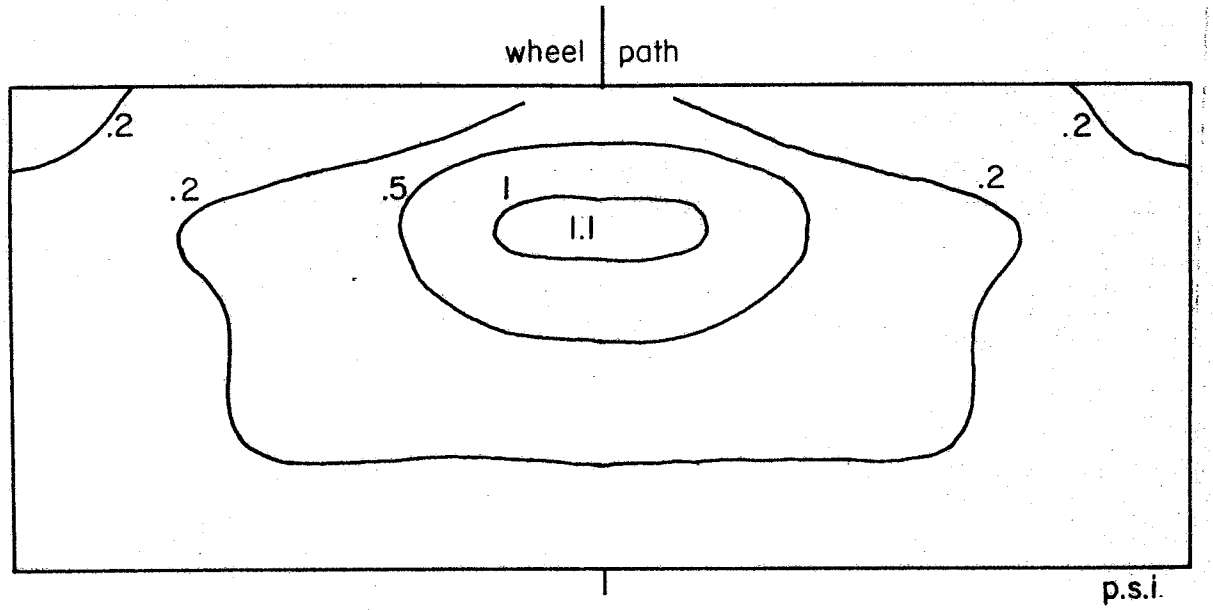

Figure 14. Cross-section of residual longitudinal stress distribution after the first pass of a 100-pound load with 50 p.s.i. contact pressure.

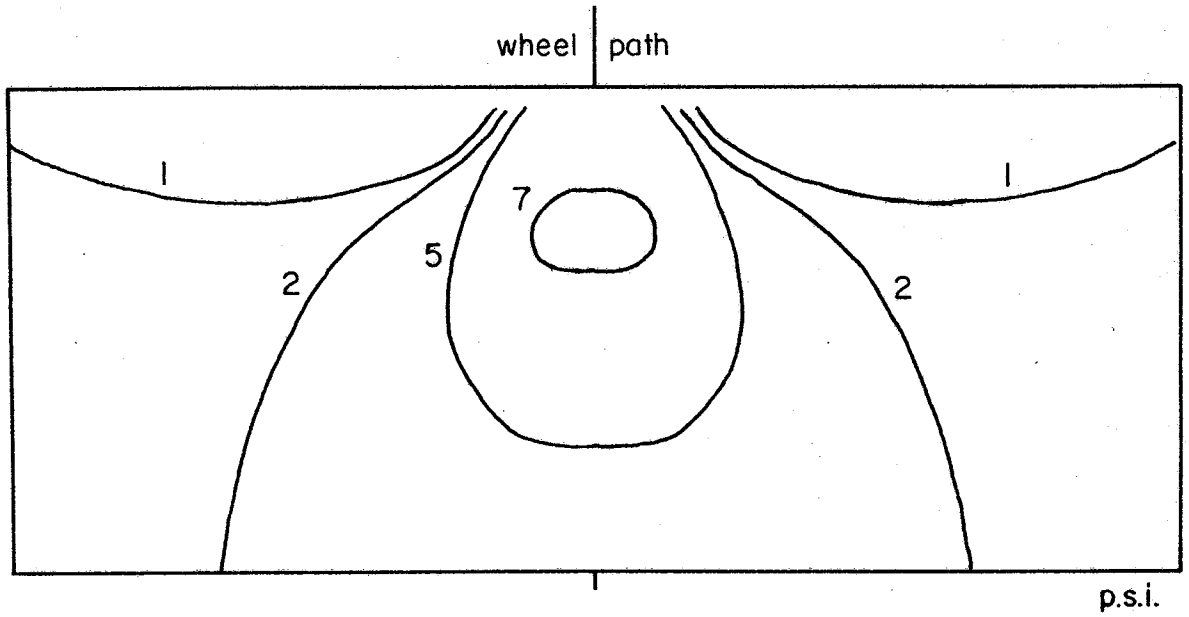

Figure 15. Cross-section of residual longitudinal stress distribution after the fifth pass of a 100-pound load with a 50 p.s.i. contact pressure.

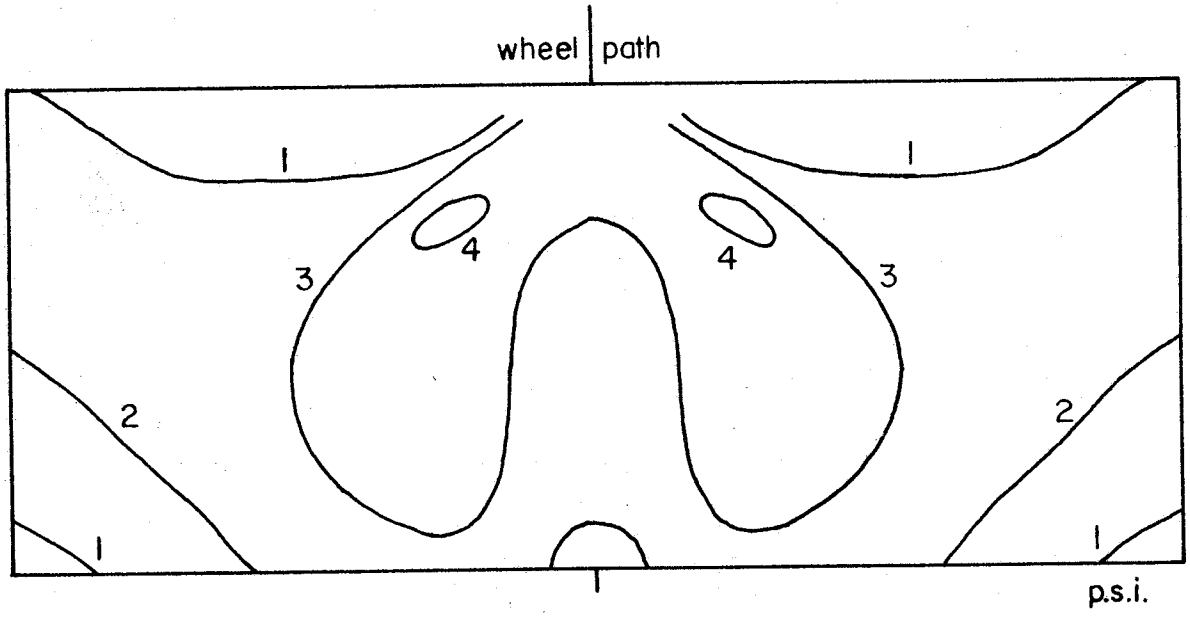

Figure 16. Cross-section of residual lateral stress distribution after the fifth pass of a 100-pound load with a 50 p.s.i. contact pressure.

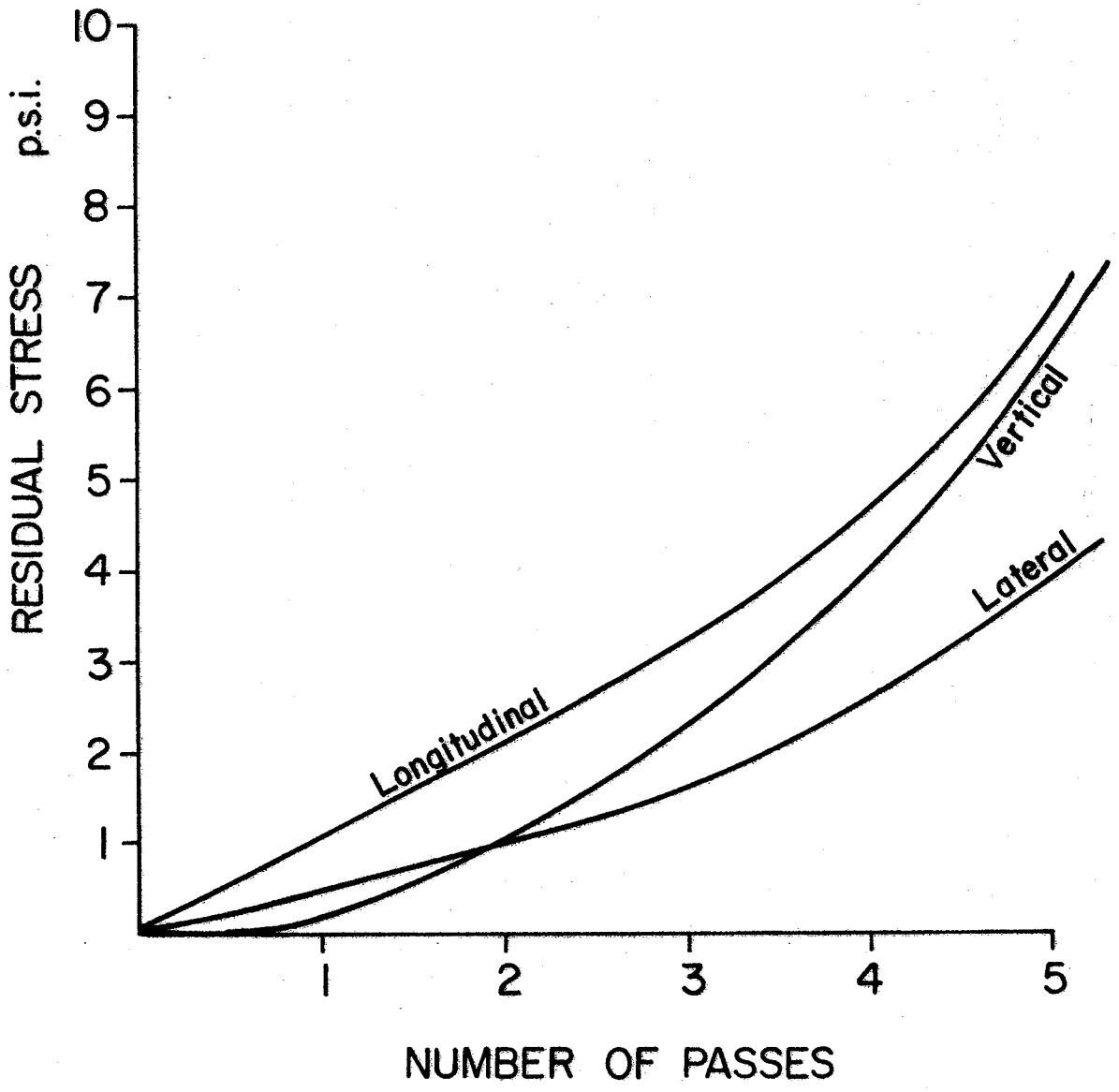

Figure 17. The increase of residual stresses with repeated one directional wheel passing.

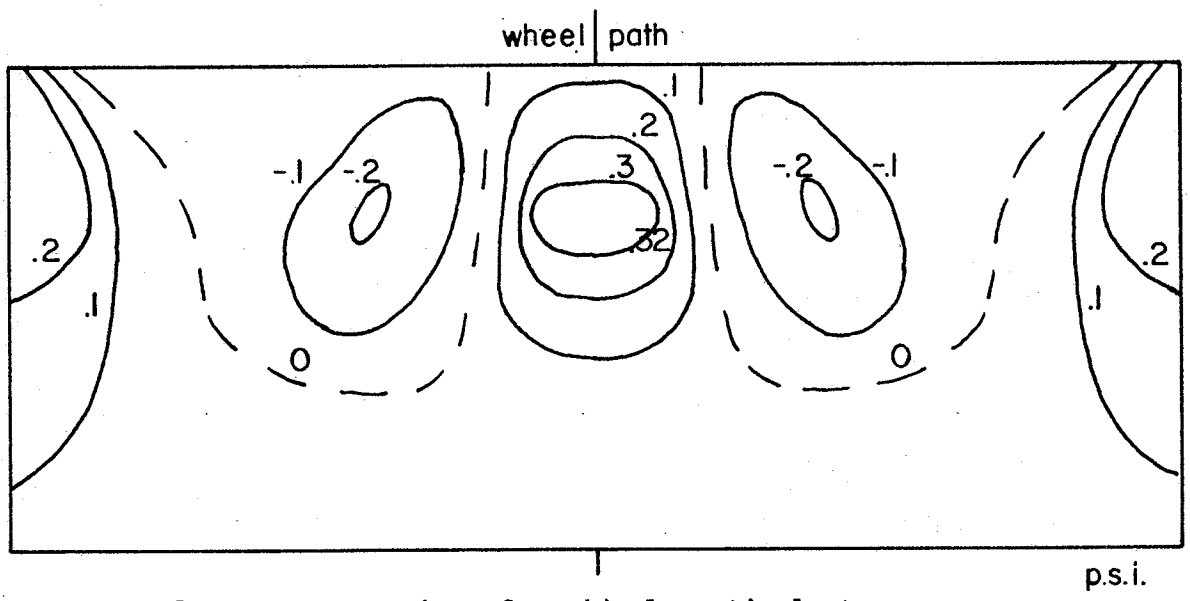

Figure 18. Cross-section of residual vertical stress distribution after the first pass of a 200-pound load with a 100 p.s.i. contact pressure.

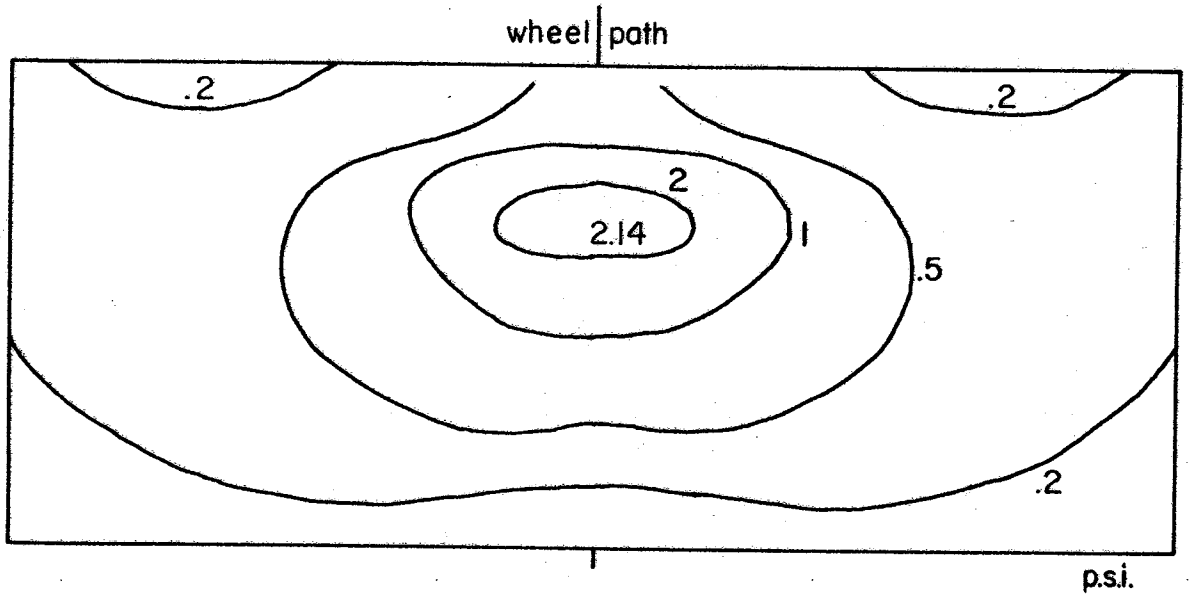

Figure 19. Cross-section of residual longitudinal stress distribution after the first pass of a 200-pound load with a 100 p.s.i. contact pressure.

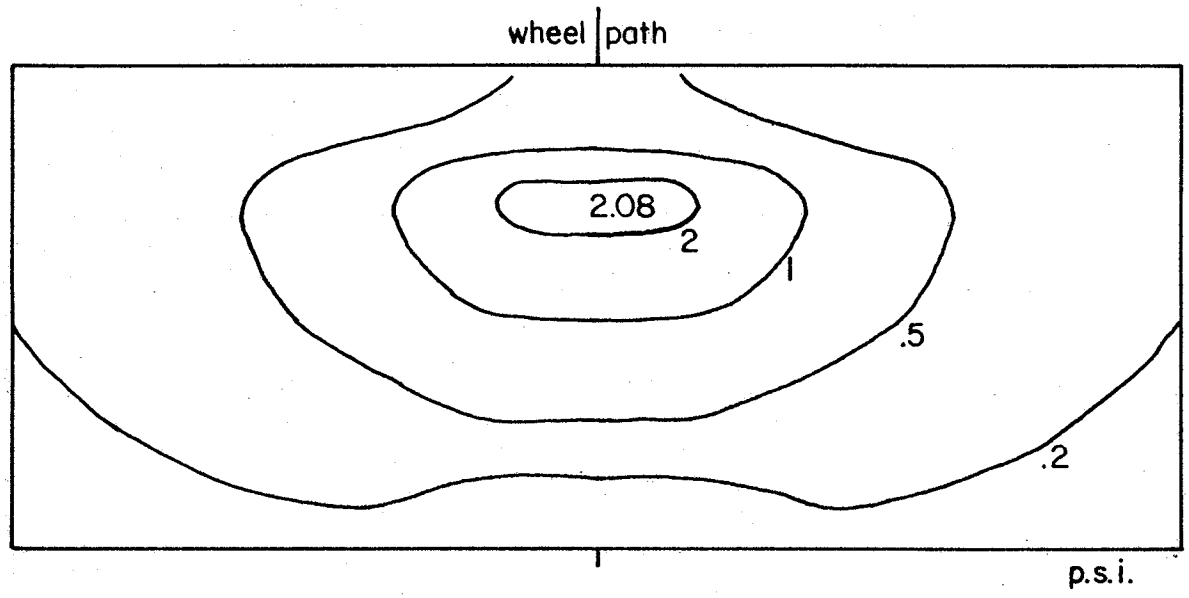

Figure 20. Cross-section of residual longitudinal stress distribution after the first pass of a 200-pound load with a 50 p.s.i. contact pressure.

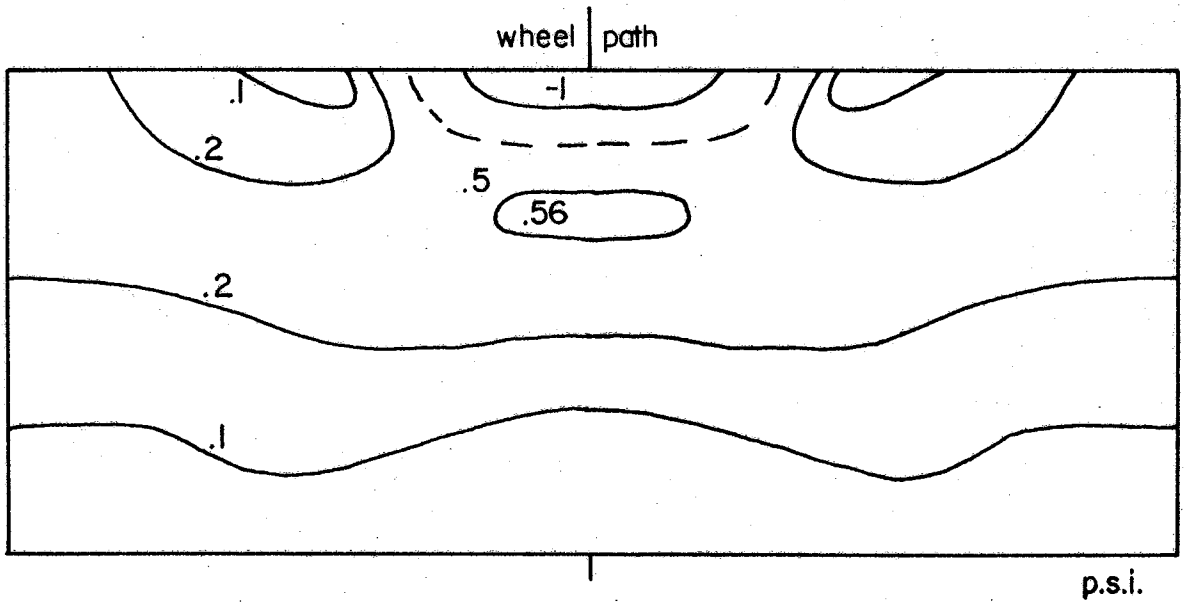

Figure 21. Cross-section of residual lateral stress distribution after the first pass of a 100-pound load with a 50 p.s.i. contact pressure.

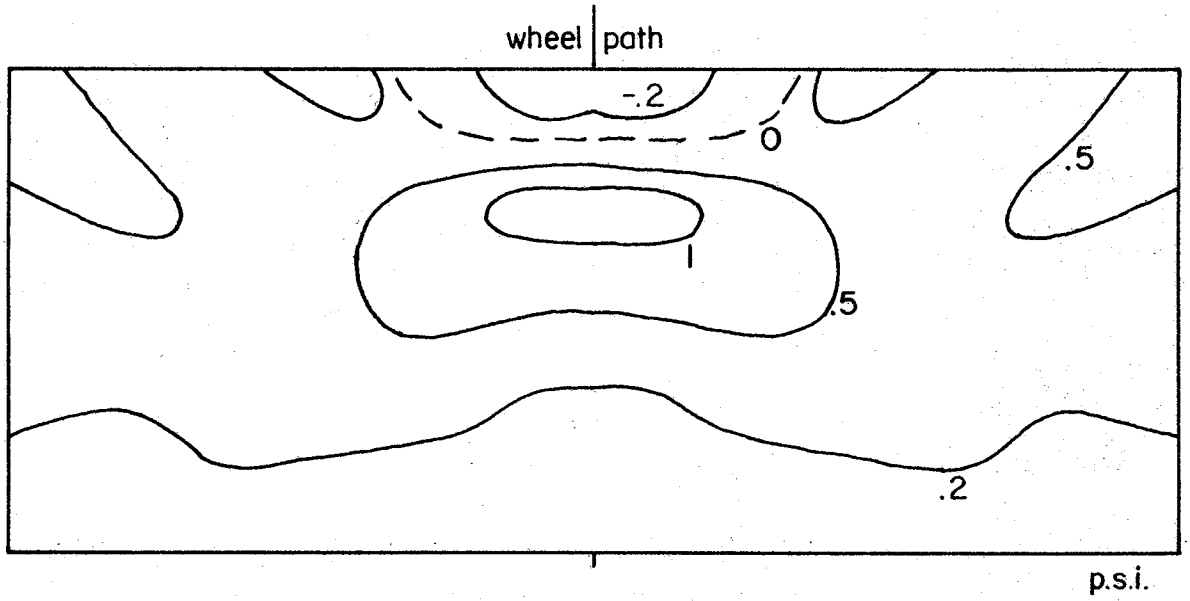

Figure 22. Cross-section of lateral stress distribution after the first pass of a 200-pound load with a 100 p.s.i. contact pressure.

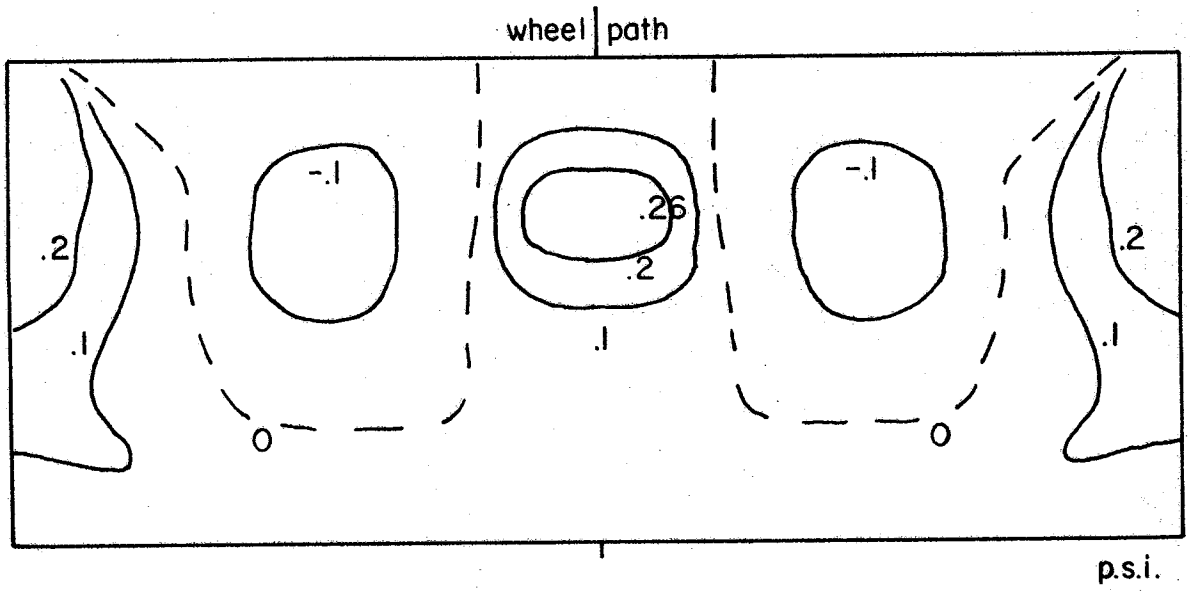

Figure 23. Cross-section of residual vertical stress distribution after the first pass of a 200-pound load with a p.s.i. contact pressure.

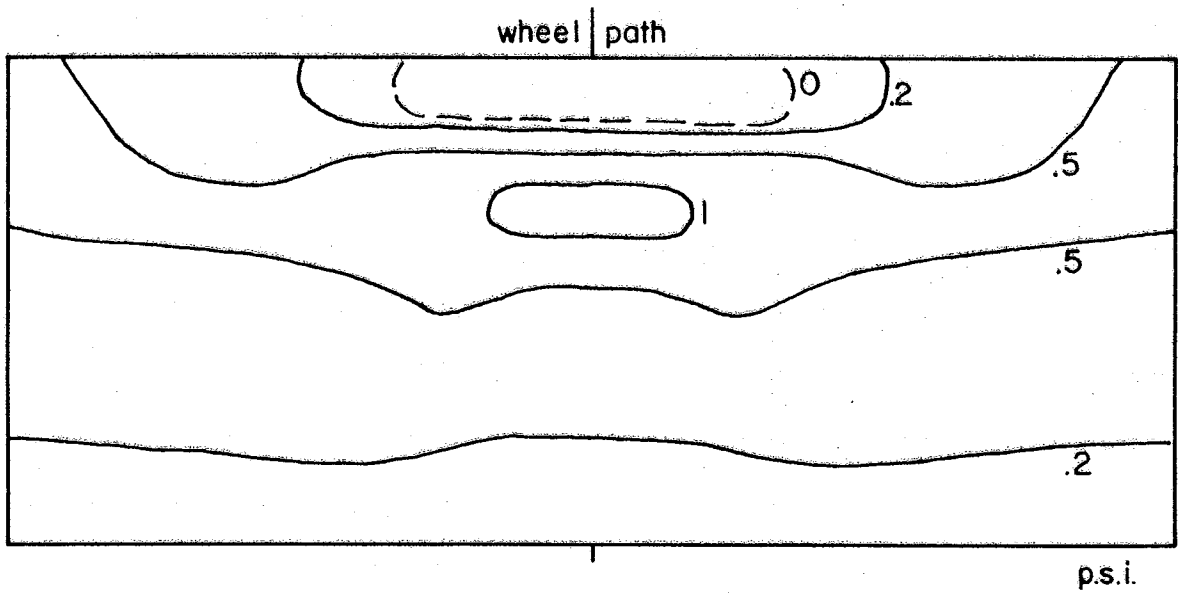

Figure 24. Cross-section of residual lateral stress distribution after the first pass of a 200-pound load with a 50 p.s.i. contact pressure.

more by increasing the vertical contact pressure than by increasing the load.

When the sides of the simulated road material are left unconfined, the vertical residual stress per pass is 17% less (Figures 12 and 25) the longitudinal residual stress is 10% less (Figures 14 and 26) and the lateral residual stress is 21% less (Figures 21 and 29) than they are with the sides restricted. This shows that the side boundary constraints of the material have some influence but are not entirely responsible for allowing residual stresses to build up. The longitudinal residual stresses will build to higher values than the other two.

(b) Transient and Residual Stresses in the Loaded Pavement

With the first passage of the 100-pound tire with 50 p.s.i. contact pressure, the cross sectional distribution of triaxial minor principal stress shows the maximum tension to be under the wheel (Figure 28) and forms a "U" shaped region of tension extending to each side of the wheel path. In the case of asphaltic material these tensions would help to decrease the fatigue life of the pavement. However after five passes (Figure 29) the build up of residual stresses has reduced the tension zone directly under the wheel by 50% but increased the tensile zones on either side of the wheel path by 50%. Thus the trend is for the critical zone to move to the surface of the pavement either side of the wheel path. This works contrary to elastic analysis results upon which modern design procedures are based.

Figure 30 shows that doubling the vertical contact stress doubles the intensity of tensile stresses in vacinity of the wheel. Figure 31 shows

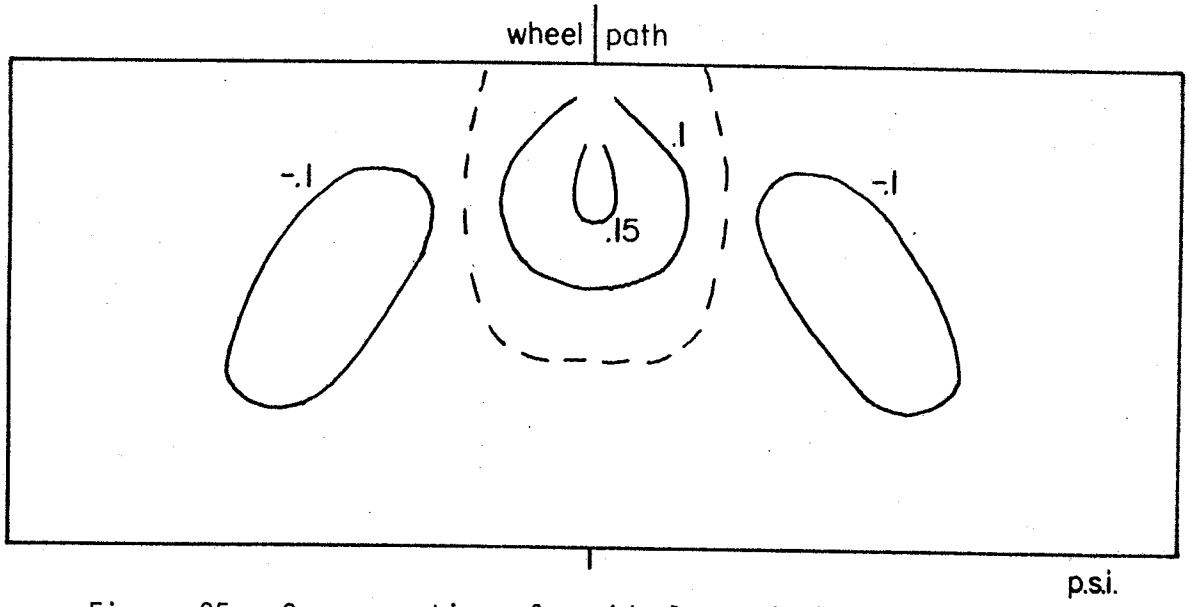

Figure 25. Cross-section of residual vertical stress distribution after the first pass of a 100-pound load with a 50 p.s.i. contact pressure with no constraints on the sides.

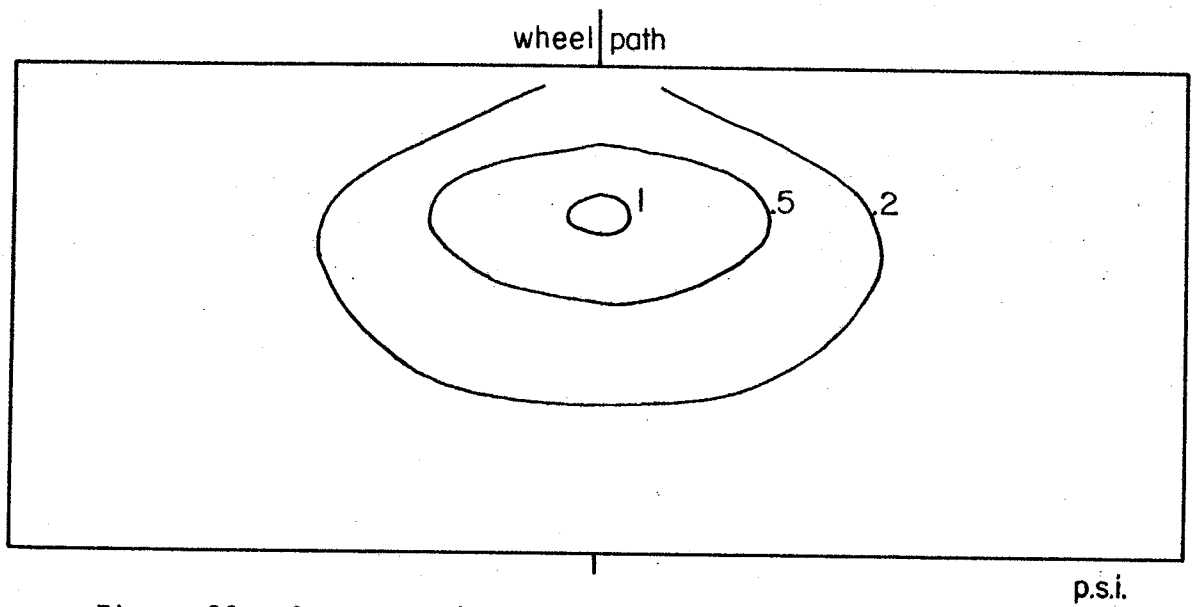

Figure 26. Cross-section of residual longitudinal stress distribution after the first pass of a 100-pound load with a 50 p.s.i. contact pressure with no constraints on the sides.

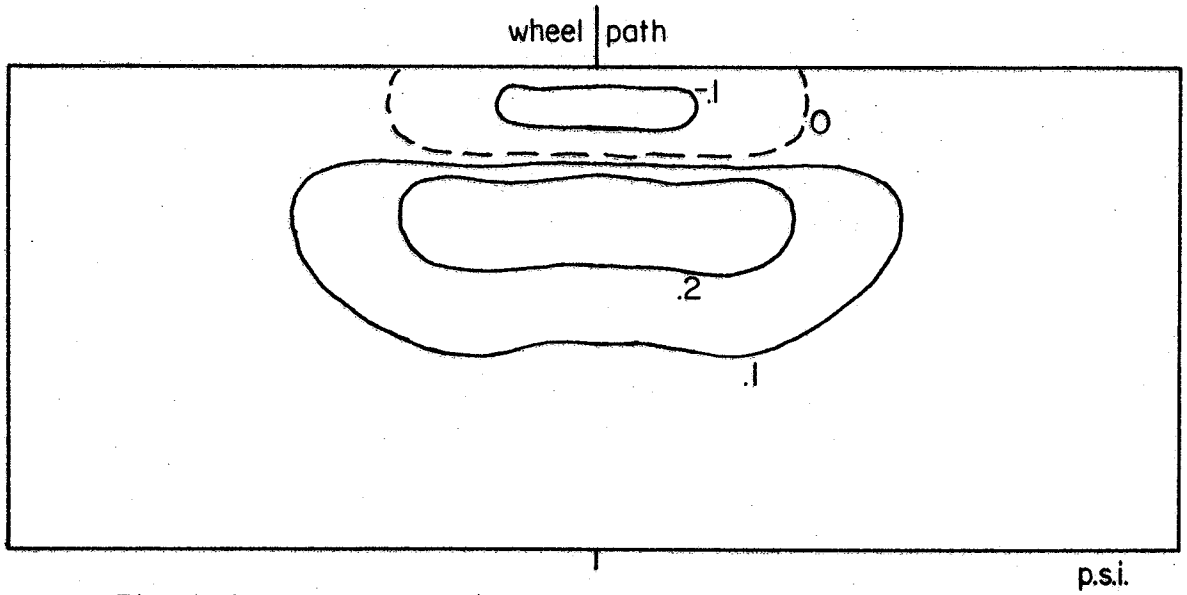

Figure 27. Cross-section of residual lateral stress distribution after the first pass of a 100-pound load with a 50 p.s.i. contact pressure with no constraints on the sides.

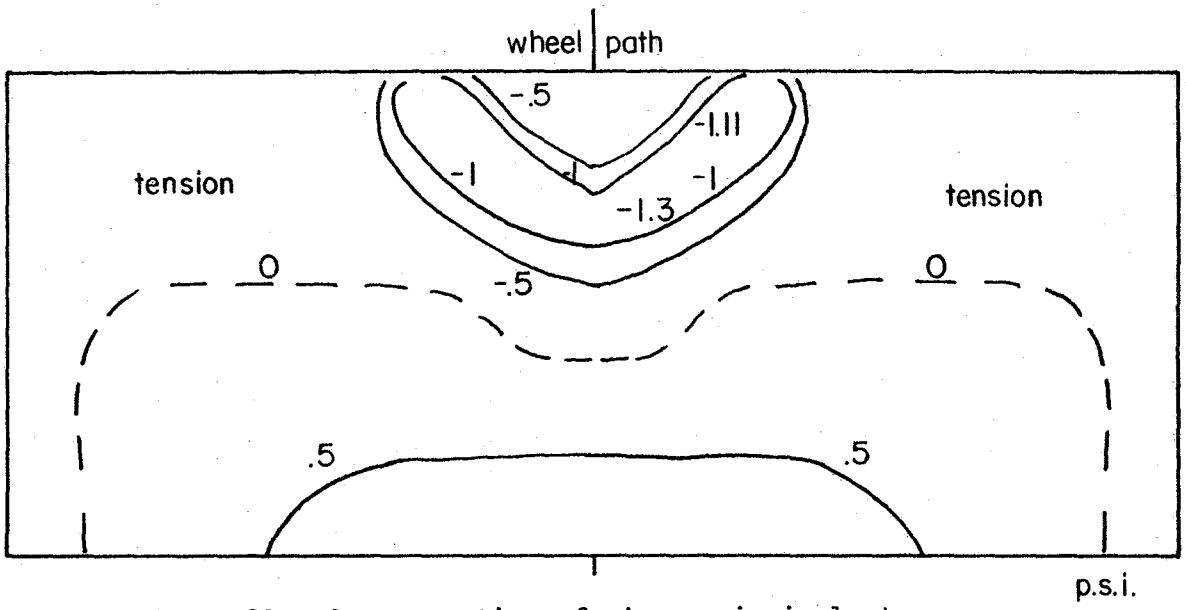

Figure 28. Cross-section of minor principal stress distribution under load during the first pass of a 100-pound load with a 50 p.s.i. contact pressure.

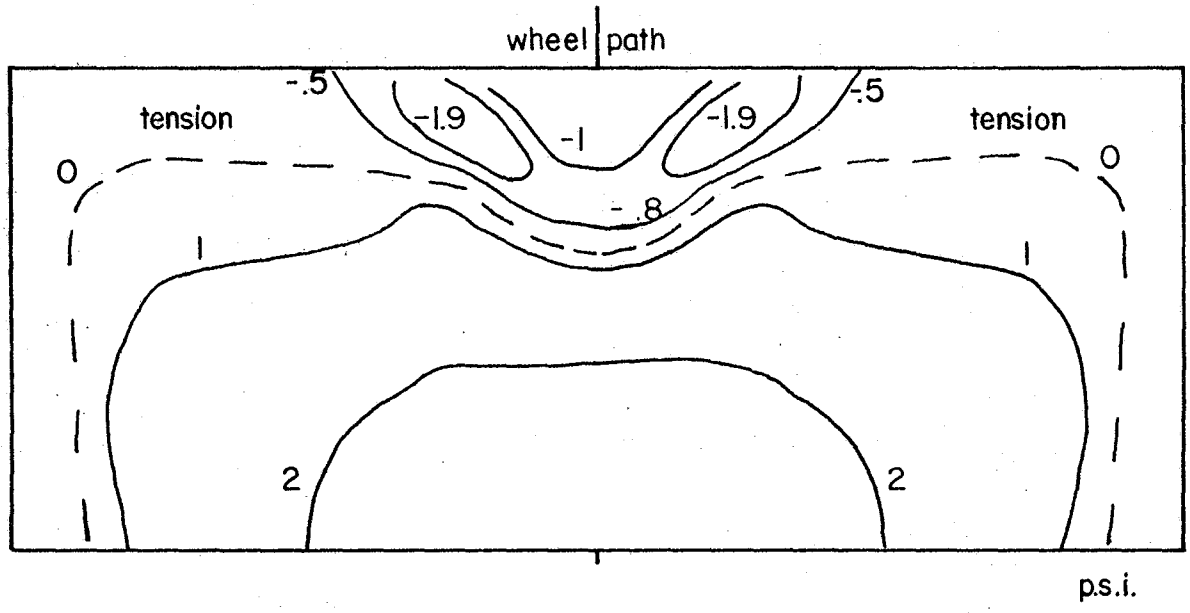

Figure 29. Cross-section of minor principal stress distribution under load during the fifth pass of a 100-pound load with a 50 p.s.i. contact pressure.

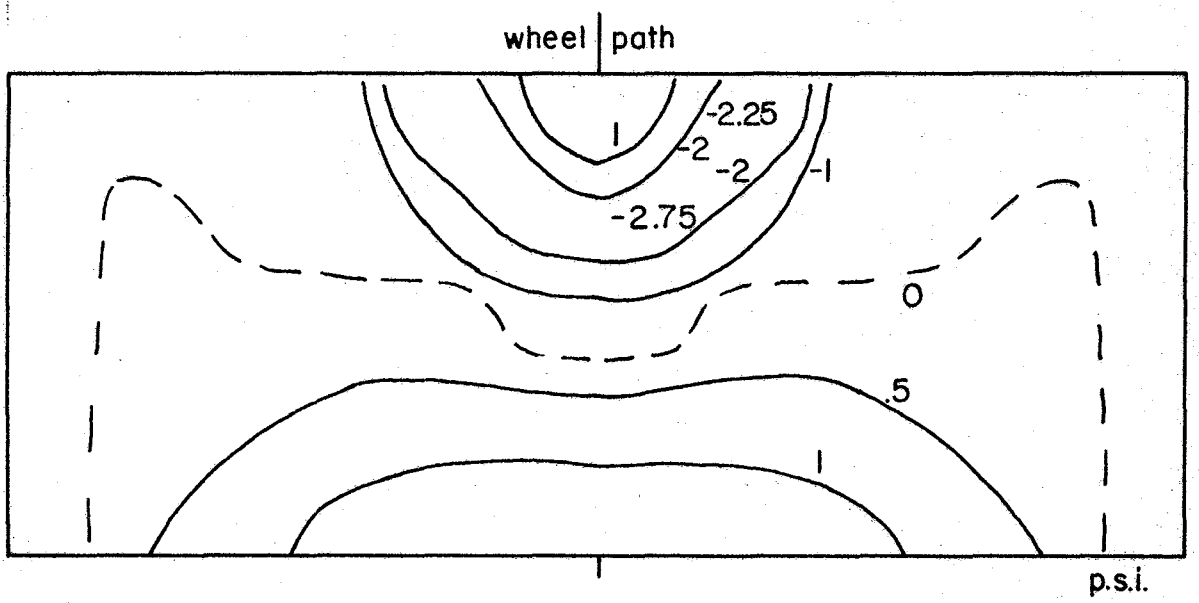

Figure 30. Cross-section of minor principal stress distribution under load during the first pass of a 200-pound load with a 100 p.s.i. contact pressure.

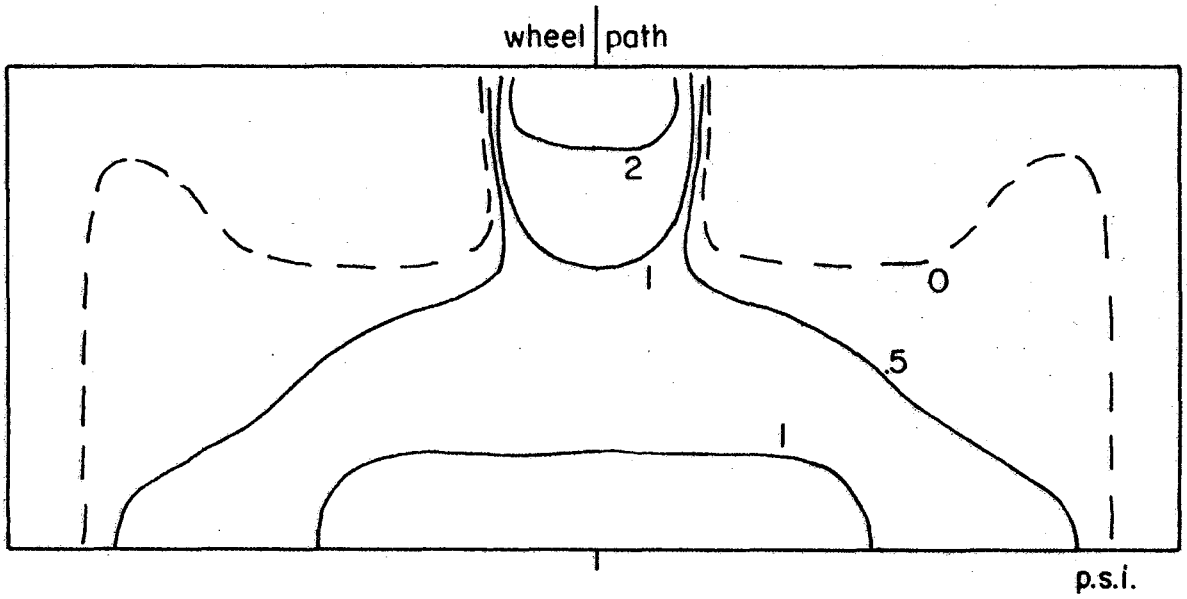

Figure 31. Cross-section of minor principal stress distribution under load during the first pass of a 200-pound load with a 50 p.s.i. contact pressure.

that doubling the contact area with a constant vertical contact stress halves the tension near the surface and eliminates it under the tire when compared with Figure 28.

When there is no side restraint the tensions under the wheel increase by 20%.

The minor principal stress patterns on vertical longitudinal sections along the wheel path are shown in Figures 32 and 33 for the first and fifth passes respectively. During the first pass equal tensions exist near the surface in front of and below the moving wheel and there are small residual tensions along the surface. After five passes the tension zones in front of and beneath the wheel have been eliminated but stresses following the wheel have increased. These comparisons demonstrate how misleading it can be to use the theory of linearized elasticity for design purposes.

Significance of Results When Strength and Modulus are Functions of Mean Stress

When the elasticity and or strength of the rolled pavement material are considered to be functions of the mean stress it is interesting to examine the effect of repeated rolling on the mean stress beneath the rolling tire.

Firstly, the increase in mean stress is evident when its cross sectional distribution under the first pass of the tire (Figure 34) is compared with that during the fifth pass (Figure 35). Some small tension near the surface deepens but elsewhere the mean stresses increase with passes, particularly beneath the rolling tire. It is fortunate that although the maximum shear stress (Figures 36 and 37), a potential cause of failure, increases with the

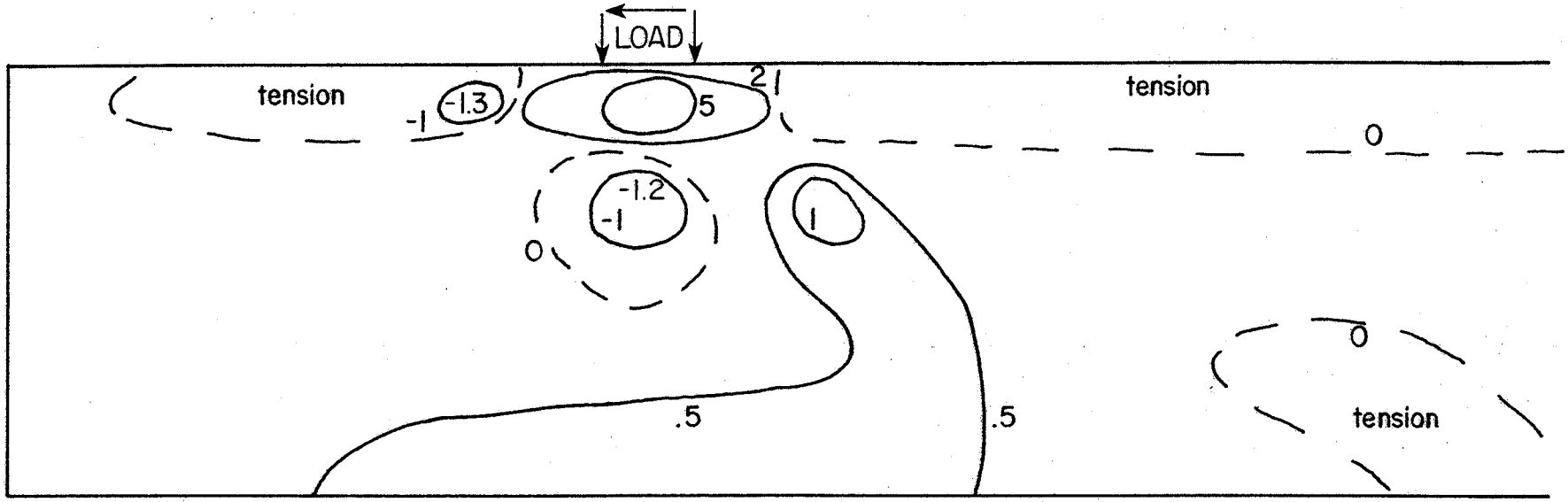

Figure 32. Longitudinal section of minor principal stress distribution during the first pass of a 100-pound load with a 50 p.s.i. contact pressure.

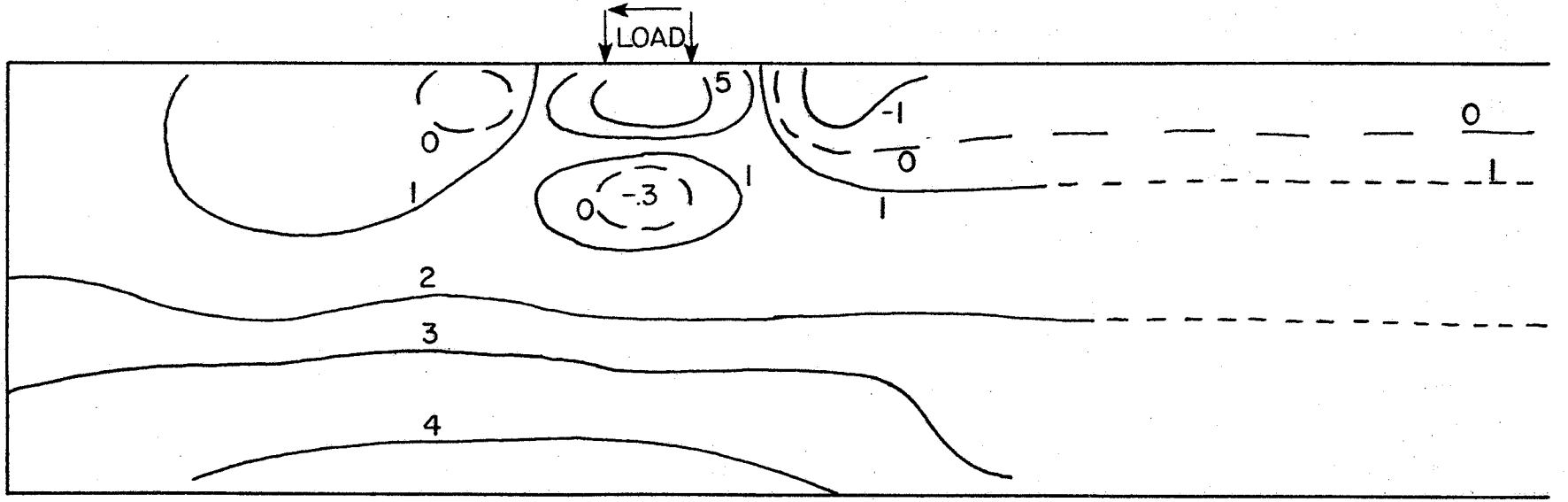

Figure 33. Longitudinal section of minor principal stress distribution during the fifth pass of a 100-pound load with a 50 p.s.i. contact pressure.

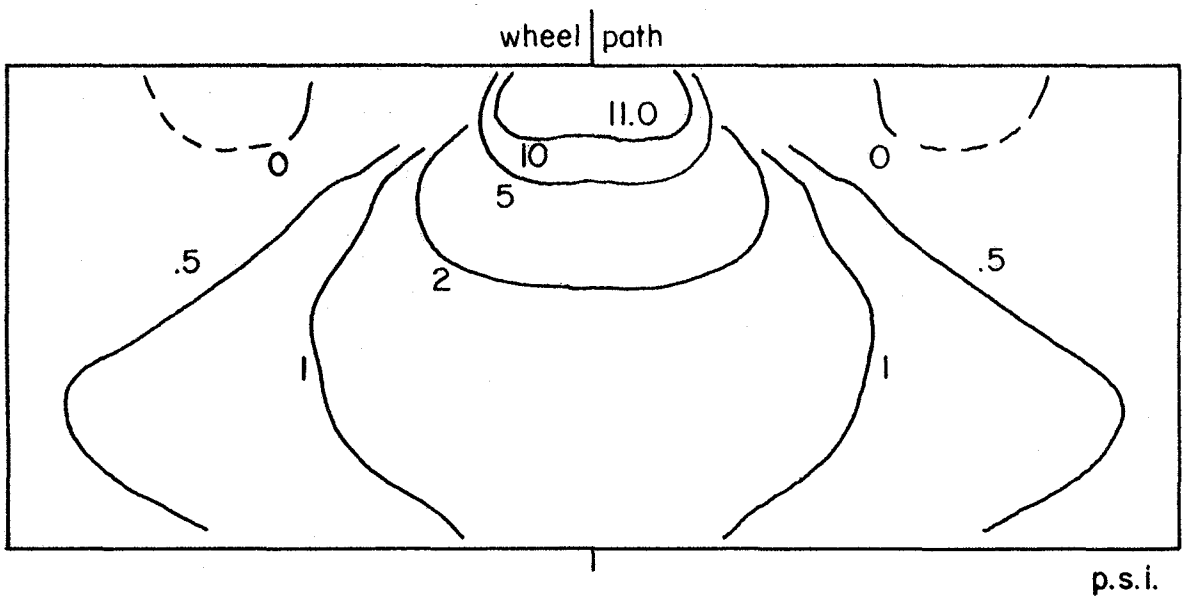

Figure 34. Cross-section of mean stress distribution under load during the first pass of a 100-pound load with a 50 p.s.i. contact pressure.

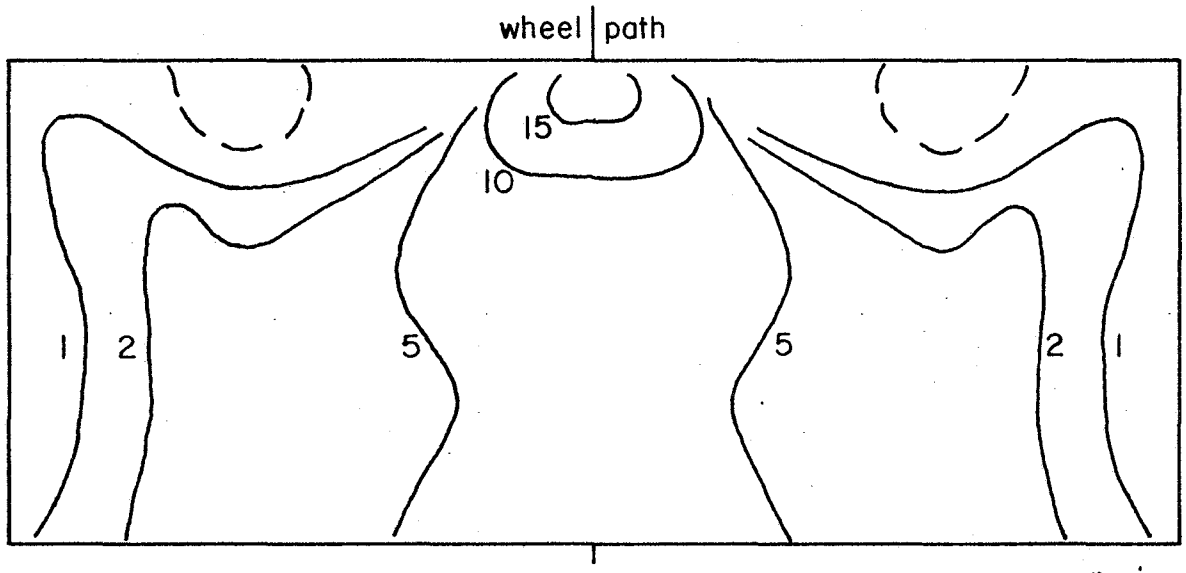

Figure 35. Cross-section of mean stress distribution under load during the fifth pass of a 100-pound load with a 50 p.s.i. contact pressure.

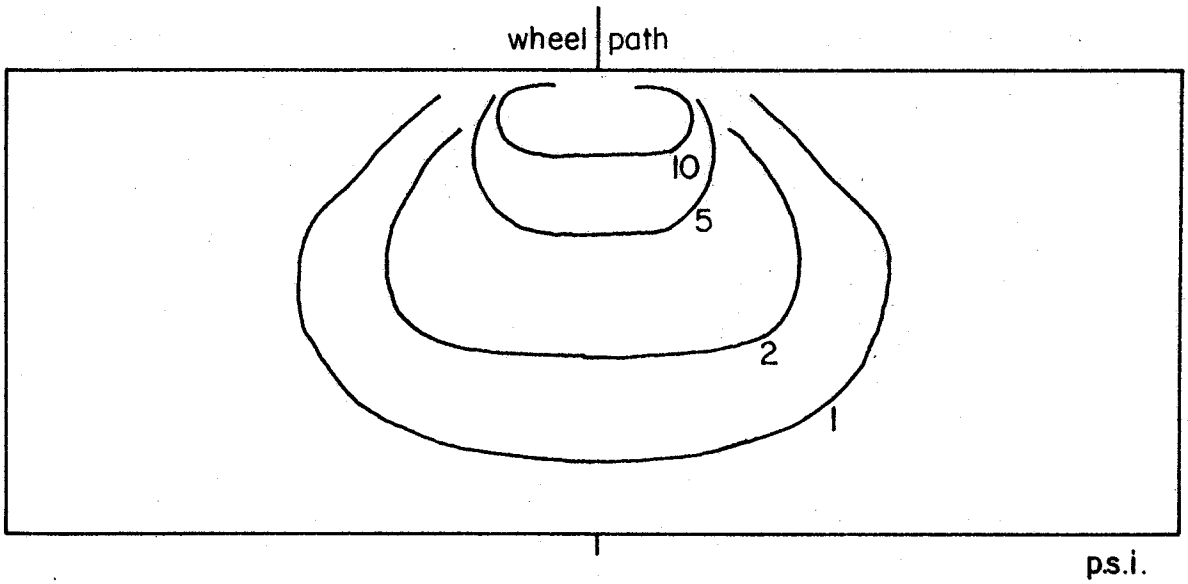

Figure 36. Cross-section of maximum shear stress distribution under load during the first pass of a 100-pound load with a 50 p.s.i. contact pressure.

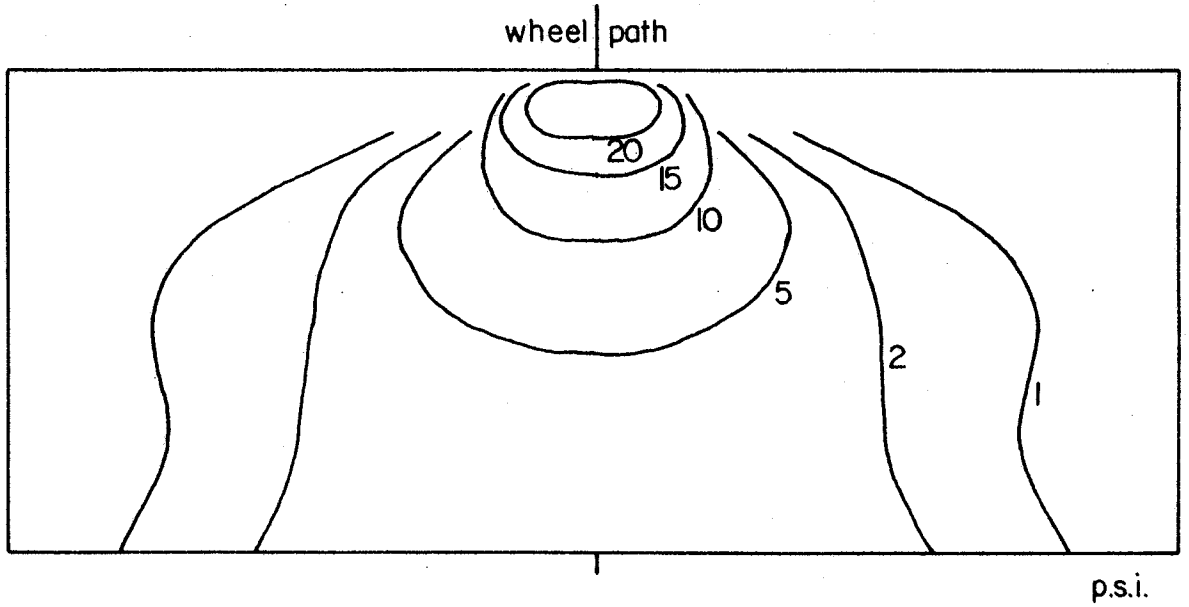

Figure 37. Cross-section of maximum shear stress distribution under load during the fifth pass of a 100-pound load with a 50 p.s.i. contact pressure.

number of passes, the increase in mean stress more than keeps pace with it; except immediately beneath and adjacent to the contact area. A judgement concerning stability made on this basis depends on the material constants in the power law. $\tau = k\sigma_{ms}^{n}$ where τ is the shear strength σ_{ms} is the mean stress k is a constant and n is a constant between 0.5 and 1.

Examination of the long-sectional distributions of mean stress and maximum shear stress shows similar results (Figures 38 and 39, Figures 40 and 41). The mean stress and hence the strength will increase in those areas where repeated rolling causes increased maximum shear stresses. This again depends on the relationship between mean stress, soil strength and rigidity parameters.

Speculation on Results

Although the analysis is of a homogenous and not a layered road structure it is possible to speculate on the way the various phenomena uncovered will influence the behavior of real pavements. For example, the behavior described above could provide some explanation for corrugations of road surfaces, rutting, and fatigue behavior.

Corrugations

Should a pneumatic tire roll with some speed along a smooth pavement made of the material under investigation and it is deflected vertically, the vertical oscillations resulting, could cause the load to vary between say 100 pounds and 200 pounds in a sinusoidal way along the pavement. The contact pressure will remain approximately constant. This analysis has shown that if the contact pressure remains constant the longitudinal flow of the material and

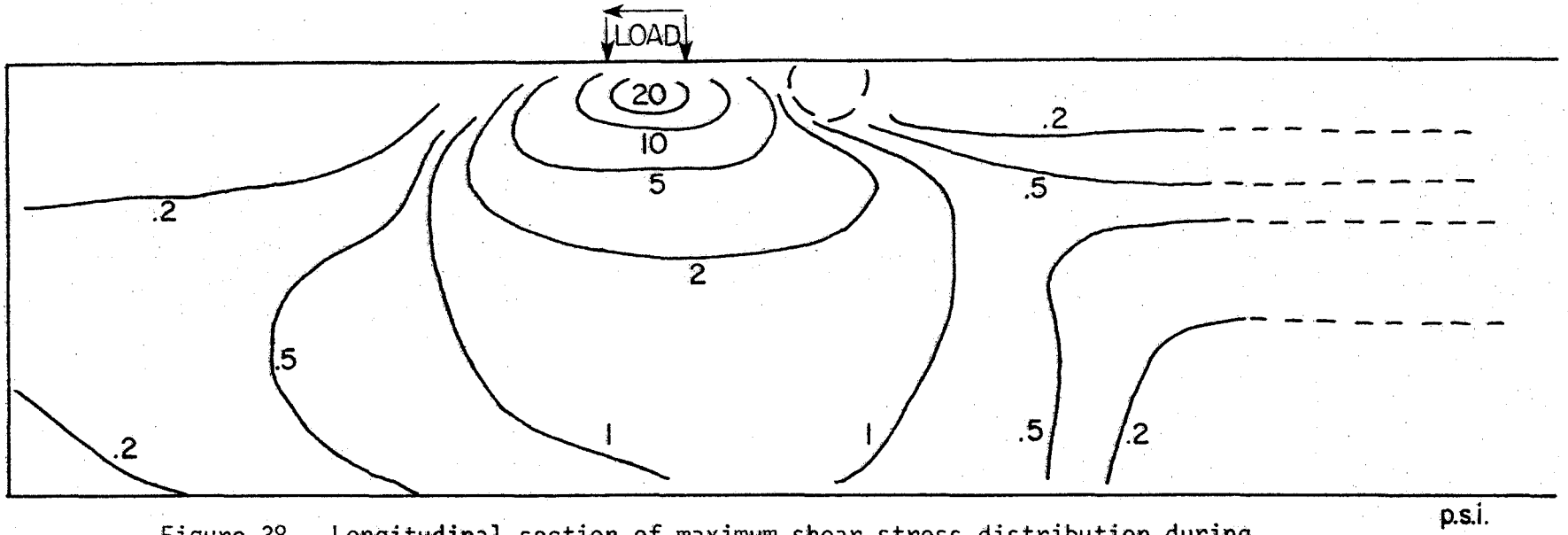

Figure 38. Longitudinal section of maximum shear stress distribution during the first pass of a 100-pound load with a 50 p.s.i. contact pressure.

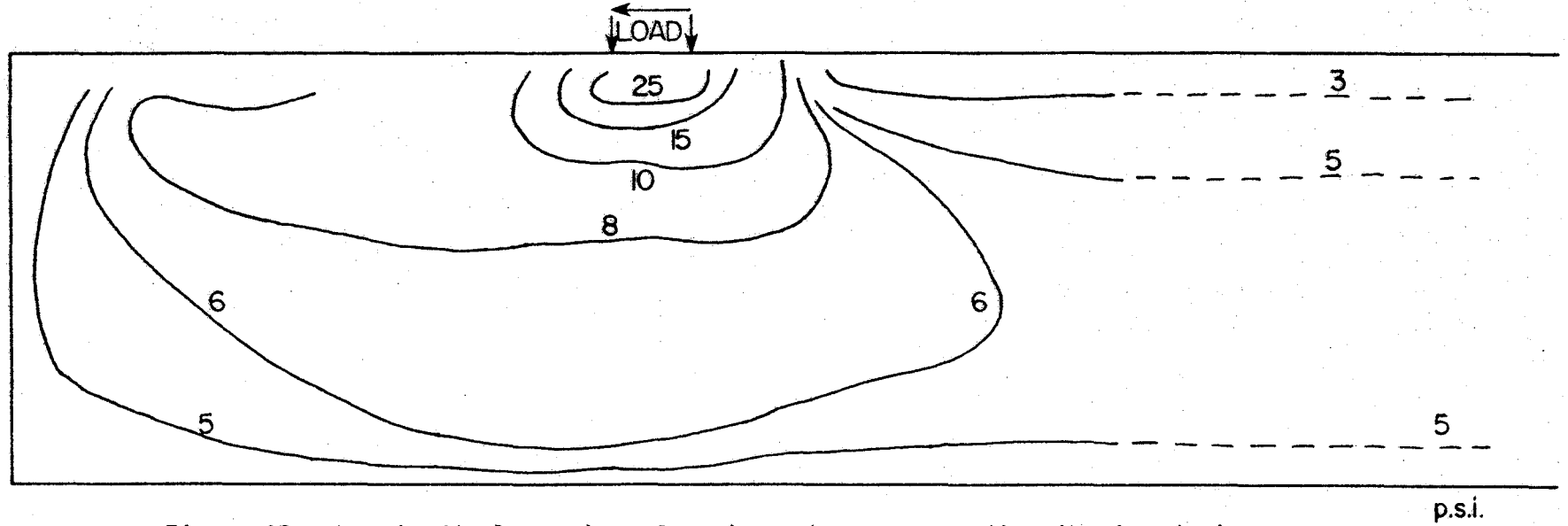

Figure 39. Longitudinal section of maximum shear stress distribution during the fifth pass of a 100-pound load with a 50 p.s.i. contact pressure.

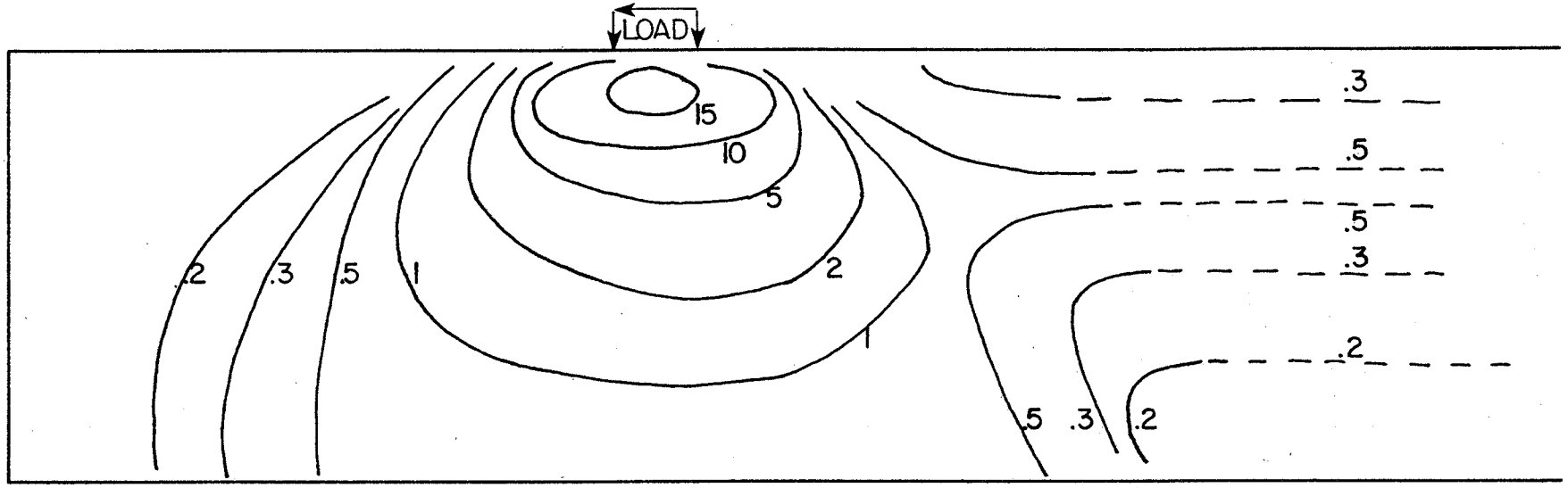

Figure 40. Longitudinal section of mean stress distribution during the first pass of a 100-pound load with a 50 p.s.i. contact pressure.

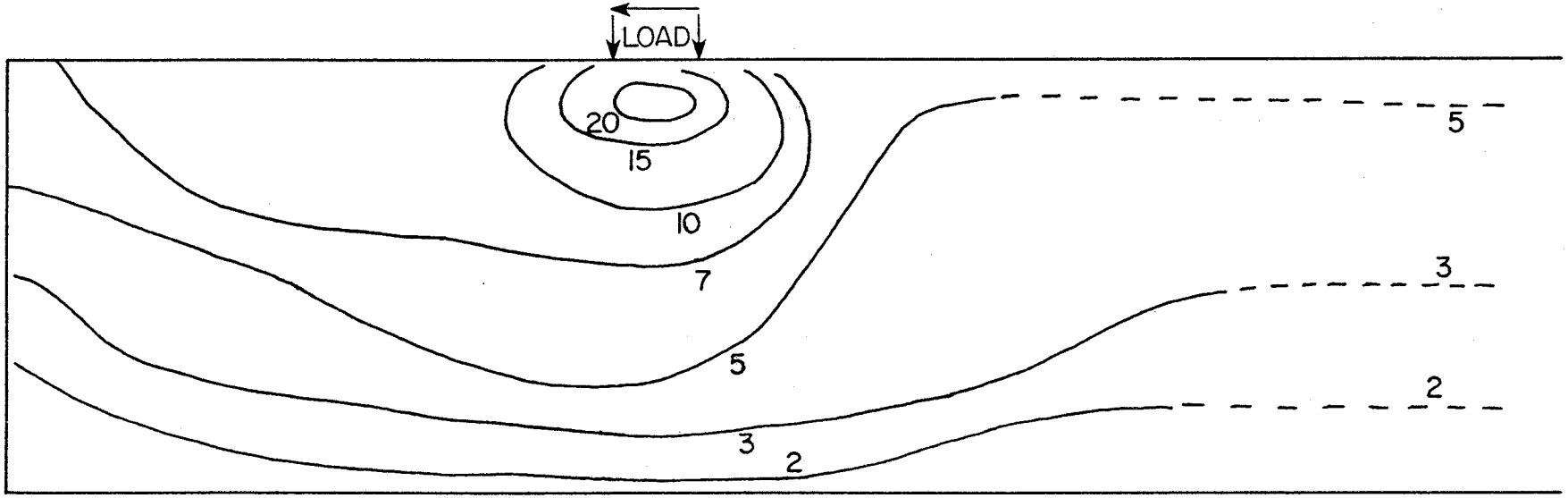

Figure 41. Longitudinal section of mean stress distribution during the fifth pass of a 100-pound load with a 50 p.s.i. contact pressure.

longitudinal residual stress build up per pass will remain constant if the material properties don't change. But the mean stress under the wheel will double each time the load rises from 100 to 200 pounds (Figures 34 and 42). If this sand clay mixture behaves as we know it does (9) the Young's Chord Modulus will be substantially higher and the plastic component lower when the repeated load is 200 pounds rather than 100 pounds. So the "strong" sections will move forward more slowly per pass blocking the passage of the faster flowing weaker materials causing the weaker material to bank up and rise still higher, forming crests at regular intervals. When repeated passes are along precisely the same track, corrugations in the bottom of the wheel rut will result. If the tracks continually change position the long transverse ridge corrugations should result.

The analysed flow of road material under one directional traffic is somewhat similar to wind action on water. The surface material will move in the direction of traffic. The deeper material will move in the opposite direction. The sinusoidal material build up will be against one side of the ridge at the surface and on the opposite side at depth tending to form vertical rotations similar to those occurring in water. Traffic forms corrugations on unsealed pavements and in hot asphaltic pavements.

Rut Deepening Predictions

The analysis has shown that rut deepening due to the unique action of one directional repeated rolling by a pneumatic tire, continues at an increasing rate provided material properties remain constant. For rut deepening per pass to slow or cease the road material must become more rigid and or less plastic. Two factors will contribute to this :

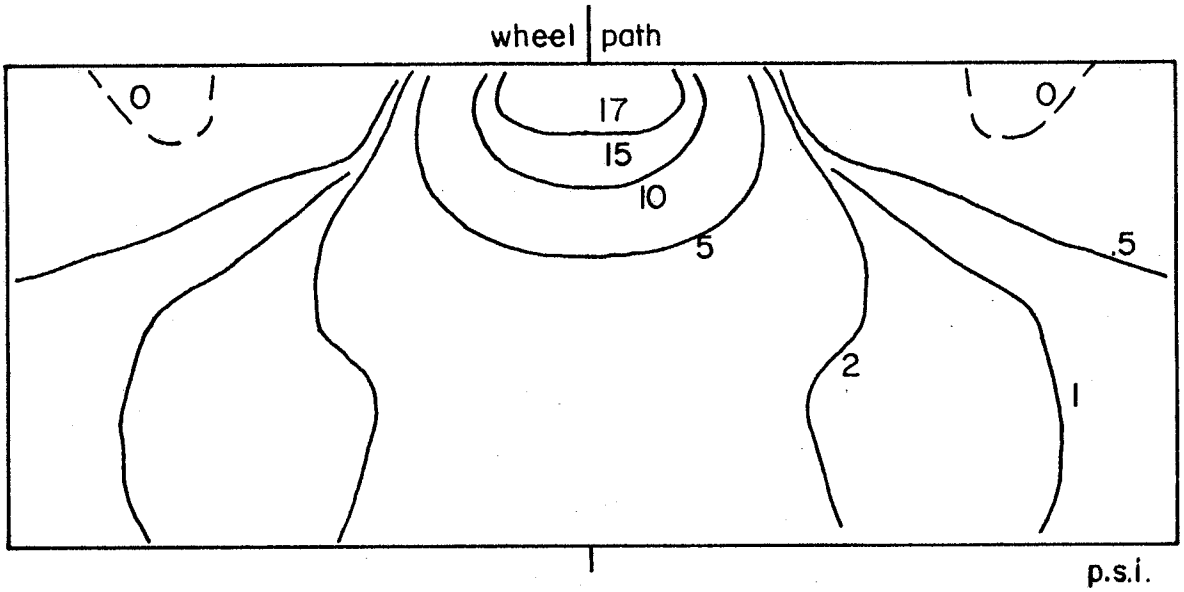

Figure 42. Cross-section of mean stress distribution under load during the first pass of a 200-pound load with a 100 p.s.i. contact pressure.

(a) The build up of residual mean stress demonstrated by this analysis will increase rigidity and decrease plasticity.

(b) The repeated rolling may cause road materials' compaction, resulting in increases in rigidity and decreases in plasticity.

To use this analysis as a means of rut prediction one would need to establish relationships between rigidity and plasticity and (i) mean stress and (ii) degree of compaction. The (i) and (ii) are progressively calculated by the three dimensional mechano-lattice analysis. So, rigorous theoretical rut prediction is possible.

The reason why some rut prediction techniques are failing (10) is because the elastic theory is used for estimating stress conditions in each layer of the pavement and for setting conditions for laboratory repeated load tests. Thus with current techniques,

(a) No account is made for residual mean stress build up as an aid to strengthening.

(b) The unique rutting action of a wheel rolling in one direction is simulated by pulse loads in the homogeneous stress conditions of repeated load traxial tests; another source of error.

Figure 43 shows a number of rut depths versus load pass curves plotted to linear but different scales for the purposes of comparison. Examination shows the curves to be of two types:

(i) Those that have a decreasing rate of rutting with passes, indicating a strengthening of material. The experiment at Nottingham (11) and the VESYS II_M predictions of Penn State's results (10) are of this type. The rate of decrease of plasticity is able to overcome the accelerating rate of rut depth increase.

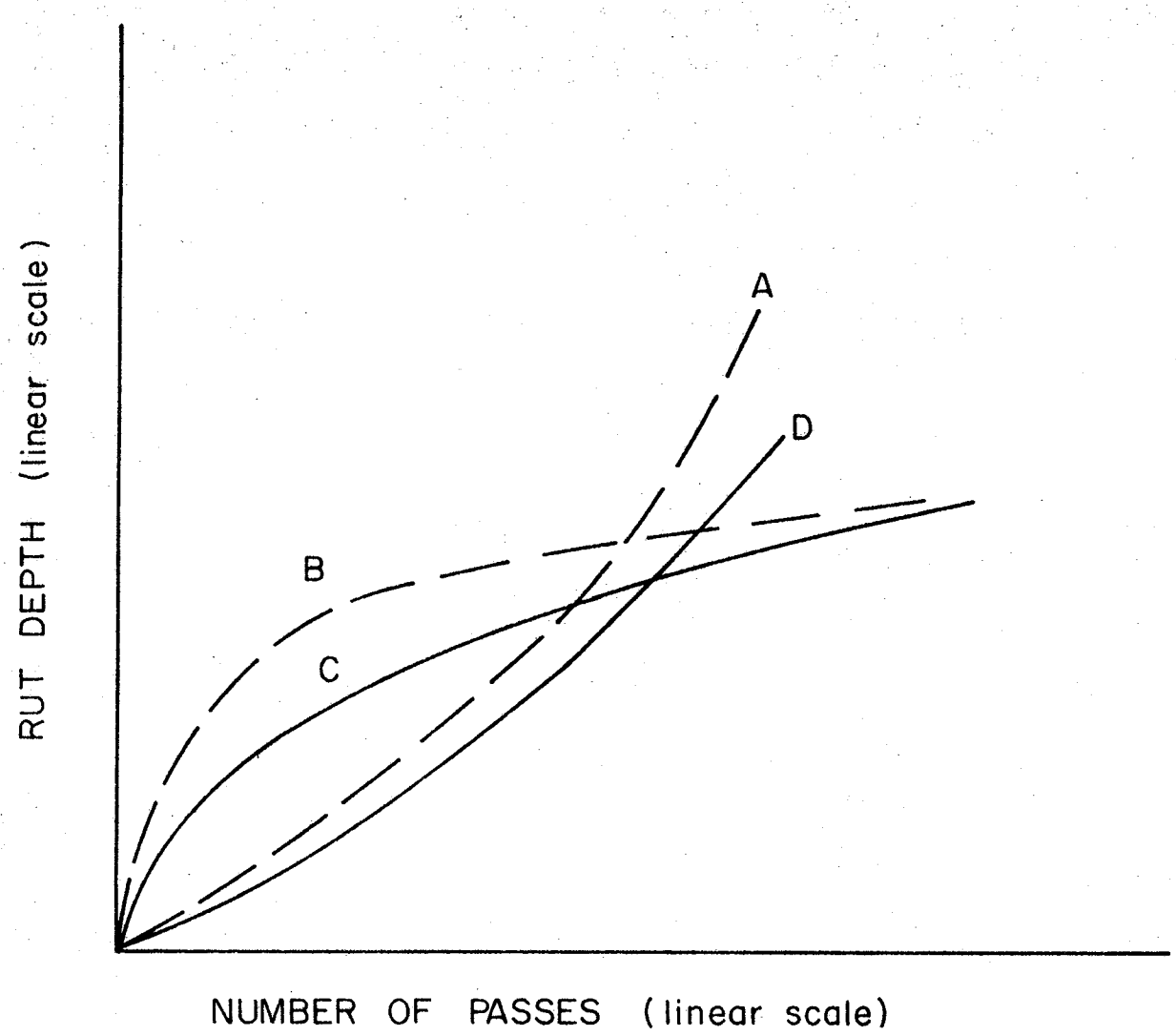

A – Experimental results from Penn State test track 2 1/2 in. bituminous surface, 4 in. bituminous concrete.

B – VESYS II predictions for Penn State results

C – Nottingham test track, 6 in. dense bituminous macadam over compacted silty clay.

D – Prediction by mechano-lattice analysis single layer of elasto-plastic material on a rigid base.

Comparison of Rates of Rut Deepening

Figure 43. Comparison of Rut Deepening.

(ii) Those that indicate an accelerating rate of rutting with passes, indicating that any material strengthening is not sufficient to overcome the natural acceleration of rutting predicted by the mechano-lattice analogy. The Penn State field test results and the mechano-lattice analysis results are of this type.

The Penn State and Nottingham test pavements are both bituminous but of different design. The Penn State results may be more realistic since wheels pass in one direction only. On the other hand the load-to-strength ratio may be too high.

It is interesting to note that the measured peak vertical permanent strain is shown in Figure 24 of (11) to move downward below the surface and intensify as passes continue, which is what one would expect if the peak vertical residual stress behaved in the same way as this analysis has shown it does in Figures 12 and 13. Figure 24 of (11) is shown in part in Figure 44 here. However, since this is a repeated elasto-plastic analysis, stress cannot be quantitatively and directly inferred from strain.

Fatigue Estimation

Most modern flexible pavement design methods include defense against fatigue failures due to repeated tension in the asphaltic layers. The multi-layer elastic analysis shows that the largest tensile strains occur in the base of the layers directly beneath the load. The elastic analysis shows that the tensile zone on the upper surface of the layers surrounding the load are less intense.

However, using the mechano-lattice analogy to represent this homogeneous material, the stress situation in the pavement is shown to

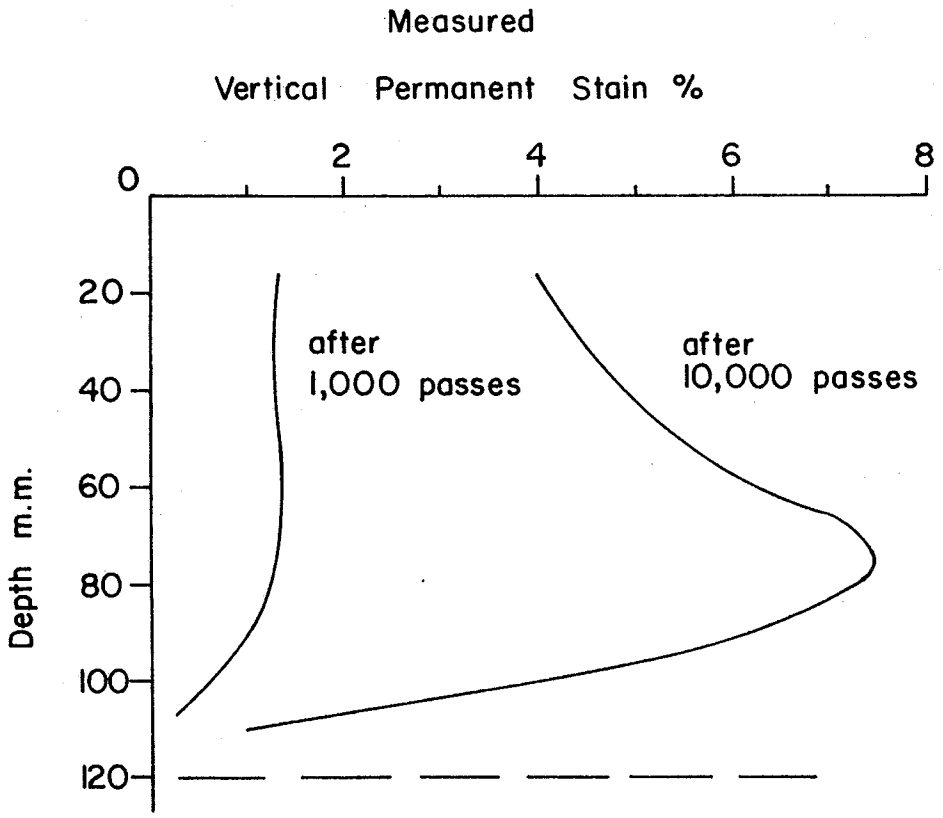

Figure 44. Measured vertical Permanent Strains in Top Layer of a Repeatedly Rolled Pavement (after Brown and Bell).

change with each wheel pass. Comparison of the triaxial minor principal stress during the first and fifth pass, shown in Figures 28, 29, 32, and 33, indicates that the tensile zones at depth under the moving wheel load are progressively reduced by repeated passing. The tensile zones on either side of the wheel on the road surface increase in intensity as wheel passing continues. This shows that multi-layer elastic analysis would probably over-estimate repeated tensile strains. In addition, the position of the zone critical to fatiguing may not be in the assumed location. The mechano-lattice analogy applied to a multi-layered structure would indicate that the position and intensity of the critical repeated tension zones may change.

One technique which would predict fatigue life versus depth in a pavement subjected to repeated passes of a particular load could be as follows:

(i) The multi-layer mechano-lattice would progressively modify the material parameters as controlled by the degree of compaction and mean stress as simulated passes continued. The parameter changes would be obtained from laboratory tests.

(ii) Laboratory fatigue tests would then be run reproducing the stress history for each depth.

(iii) The failures indicated by the laboratory fatigue tests would then be incorporated in the analysis so that the sequence of events during failure could be predicted.

The above accurate but expensive technique could be simplified greatly to give appropriate accuracy to fatigue life prediction and still be in principal superior to techniques in current use.

REFLECTION CRACKING IN OVERLAYS

Introduction

The familiar problem of reflection cracking in overlays can be analyzed using the mechano-lattice analogy three dimensional plane strain analysis. The problem is of a different nature to the traveling stress problem of a rolling wheel. The overlay is subjected to repeated tensile strain pulse cycles due to expansion and contraction of a cracked underlying pavement. Consequently, the calculated stages of stress history must be stored in separate sets of arrays. For this problem only two sets of arrays are used; one for the underlying crack closed, the other for the underlying crack open.

The material behavior was estimated from the results of laboratory repeated tensioning tests with a 3" X 3" X 15" bar of asphalt overlay bonded on one side to a two part platen (See TTI Research Report 207-5). The platen pieces were drawn apart 0.07" and closed repeatedly. The load-deflection curves were plotted by an x-y recorder. Figure 45 gives typical results for the third, tenth, and hundredth cycle. At early stages of repeated straining the load-unload path can be approximated by a triangle, the loading side having four times the compliance of the unloading side. When stress is reversed the same load-unload path is repeated to approximately close a parallelogram shaped loop. The increasing tension and increasing compression modulus was assumed to be 30,000 p.s.i. The decreasing tension and decreasing compression modulus was four times that at 120,000 p.s.i. The mechano-lattice analogy analysis is for plane strain of a 4" thick overlay with the top 22" surface free to move and with a one inch distance on each

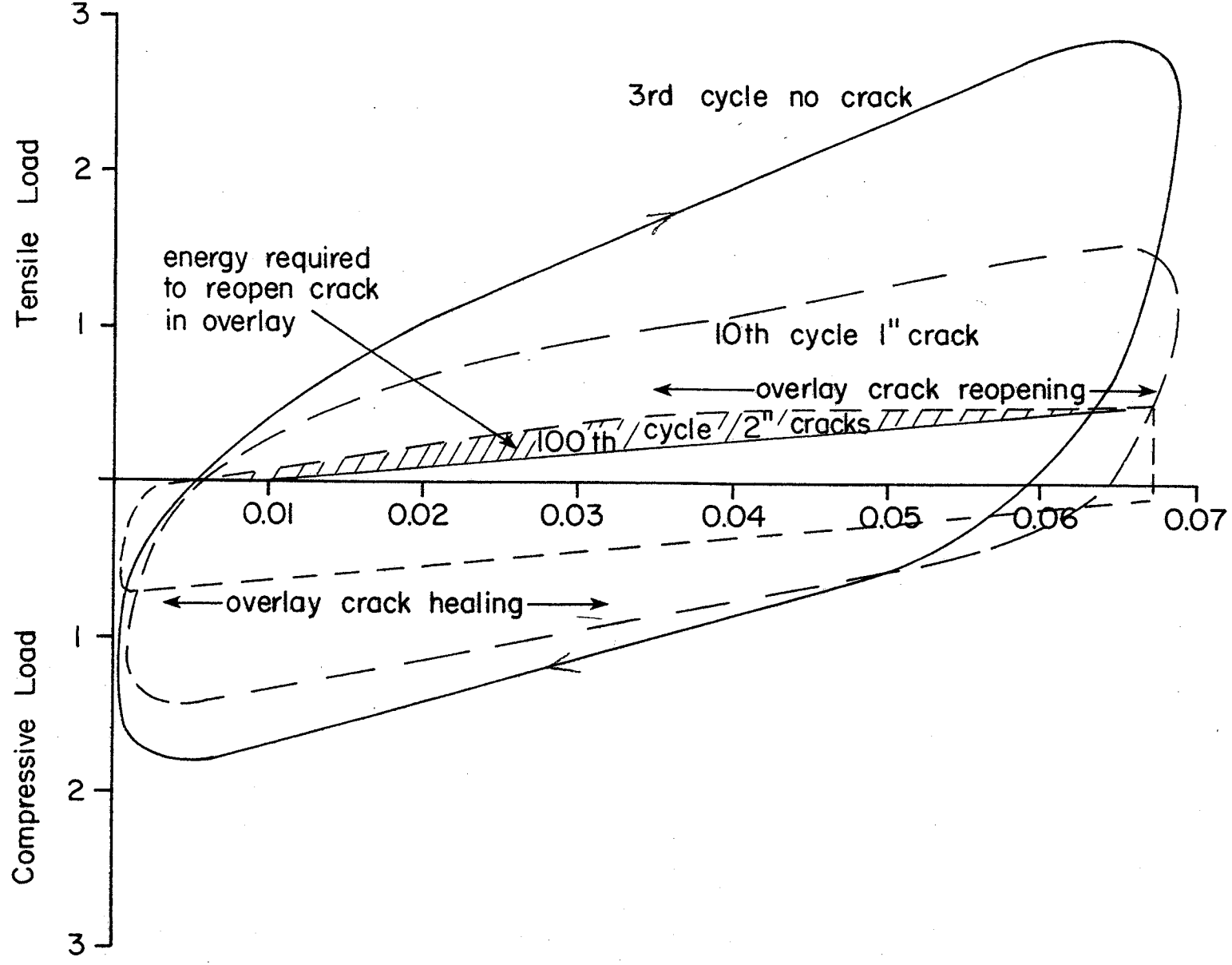

Figure 45. A load-deflection plot of a repeated crack opening under an overlay in the laboratory.

side of the crack where the overlay and the old pavement are debonded.

Results

Stresses

Figures 46 through 50 show the patterns of calculated vertical, longitudinal, lateral, minor principal, and shear stresses for the first pull to 0.07 inches. The maximum longitudinal and maximum minor principal stresses of -1030 p.s.i. (tensile) and -1044 p.s.i. respectively occur on the lower side near the simulated crack.

The stress distribution for the first closing of the crack is shown in Figure 51 through 55. Once the crack is closed again, substantial compressive stresses exist where before straining there were none. So they can be viewed as a type of residual stress. The maximum longitudinal compression is smaller in magnitude than the first maxumum tension. The stress distribution for the second opening and for the second closing are shown in Figures 56 through 60 and 61 through 65 respectively.

The maximum longitudinal tensions and compressions at no deflection, first opening, first closing, second opening, and second closing are shown plotted in Figure 66. If these results had been plotted from a uniaxial repeated tension-compression test with 0.02 inches extension over a two-inch long sample, the first tensile loading modulus would be 29,400 p.s.i., the first unloading modulus would be 120,000 p.s.i. These are very close to the assumed moduli used in the analysis. Figure 66 shows that after about four tension-compression cycles, the maximum tension will continue to be about 700 p.s.i. (compared with 1030 p.s.i. for the first pull) and

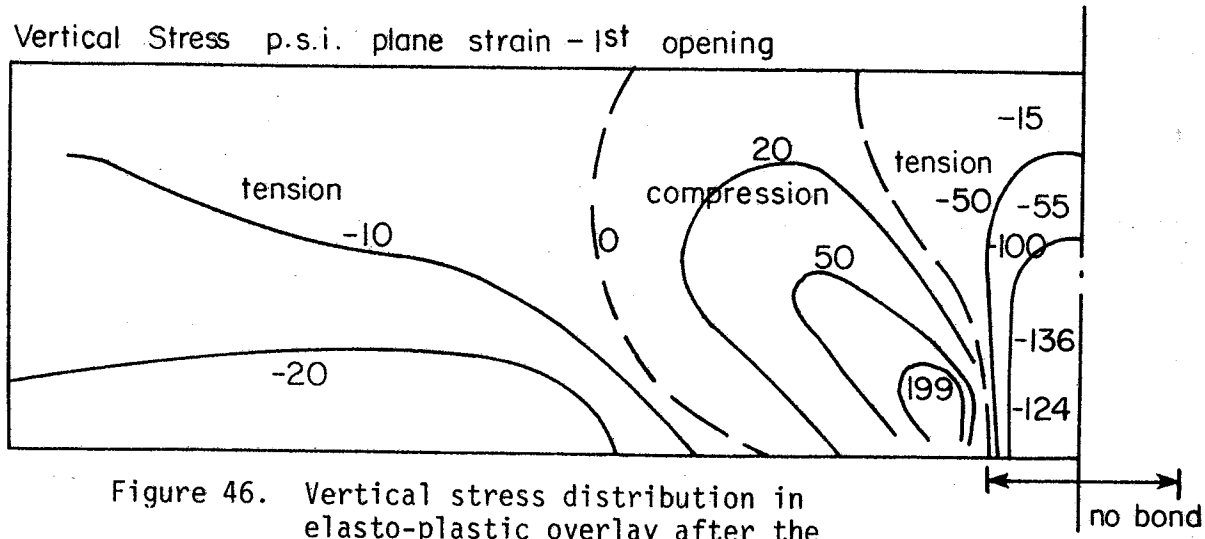

Figure 46. Vertical stress distribution in elasto-plastic overlay after the first 0.07 inch crack opening.

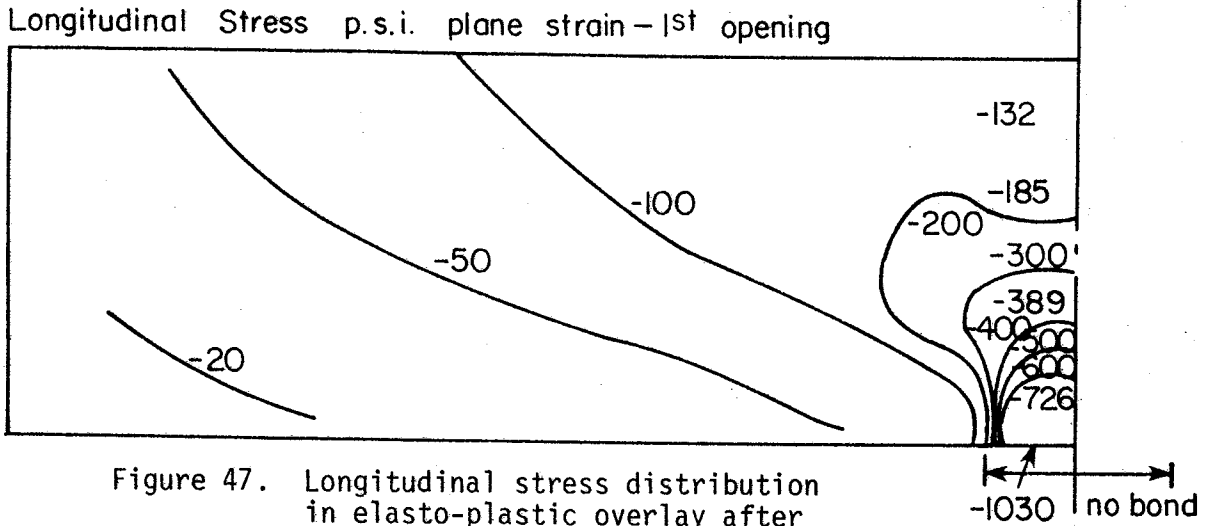

Figure 47. Longitudinal stress distribution in elasto-plastic overlay after the first 0.07 inch crack opening.

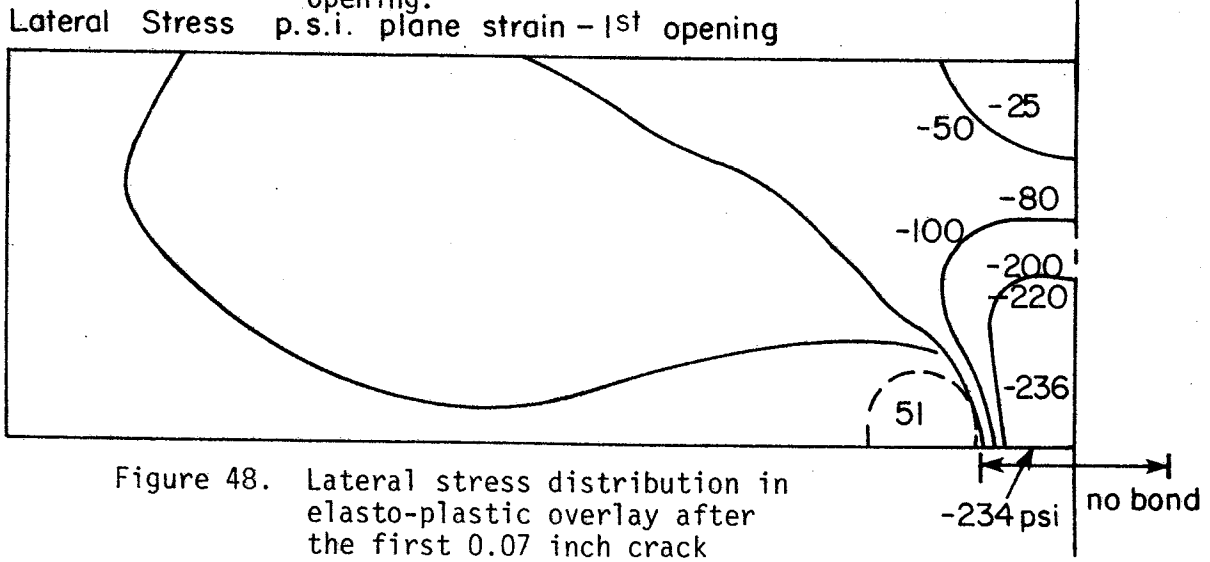

Figure 48. Lateral stress distribution in elasto-plastic overlay after the first 0.07 inch crack opening.

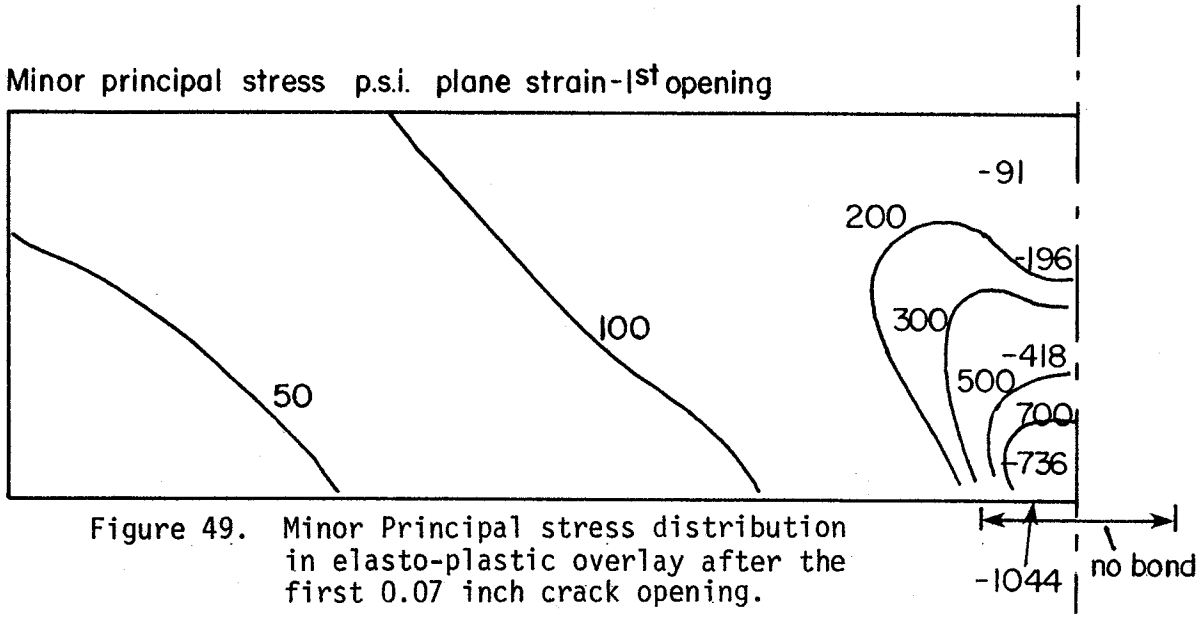

Figure 49. Minor Principal stress distribution in elasto-plastic overlay after the first 0.07 inch crack opening.

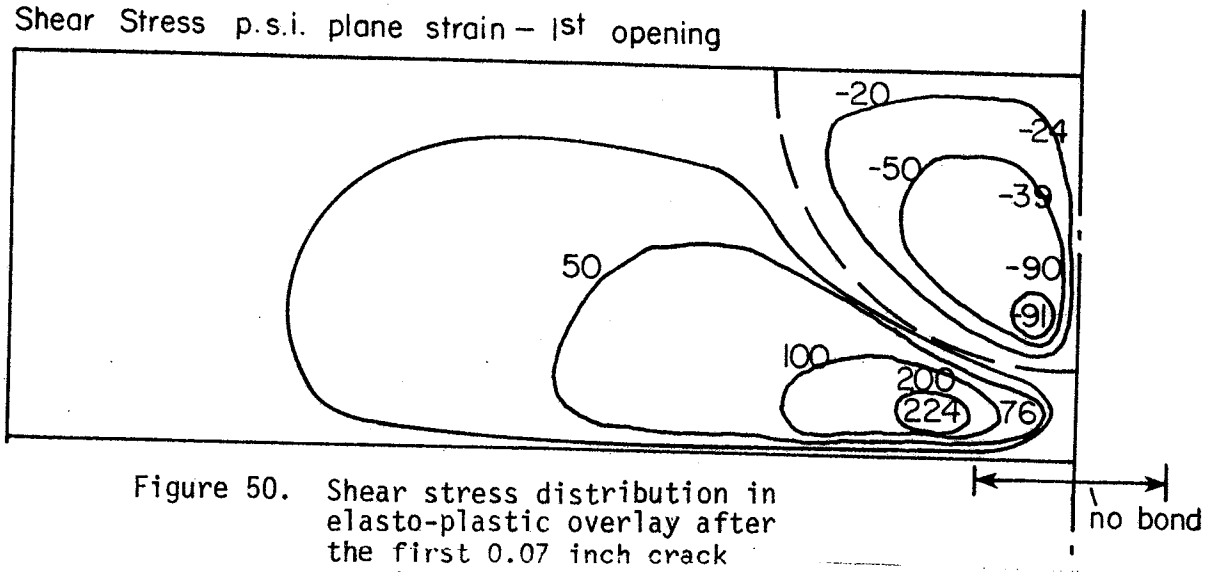

Figure 50. Shear stress distribution in elasto-plastic overlay after the first 0.07 inch crack opening.

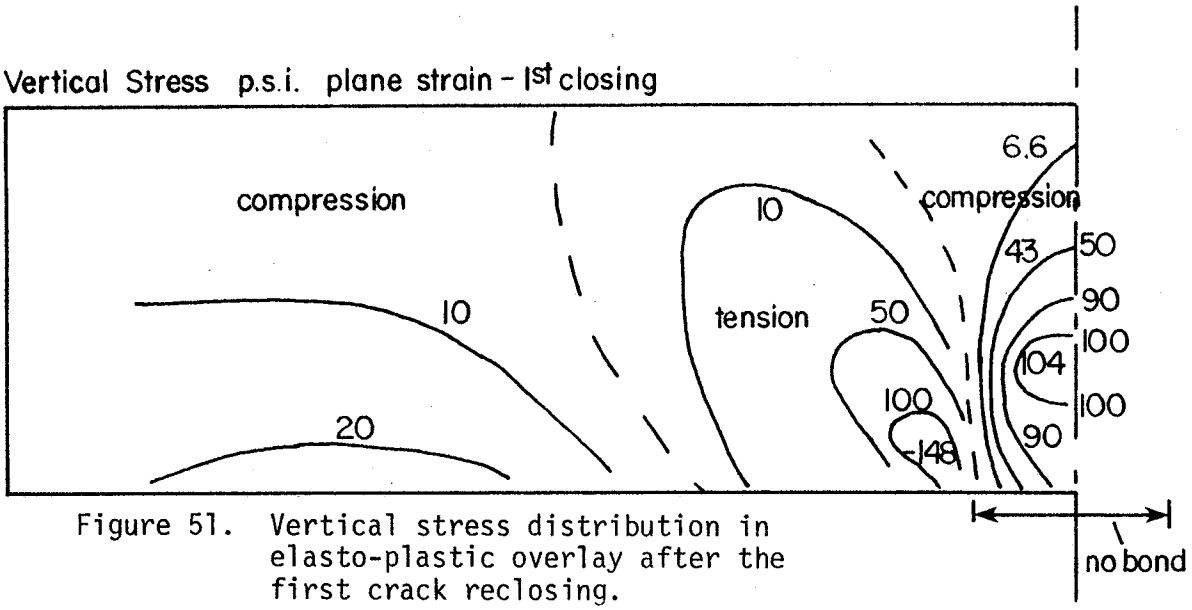

Figure 51. Vertical stress distribution in elasto-plastic overlay after the first crack reclosing.

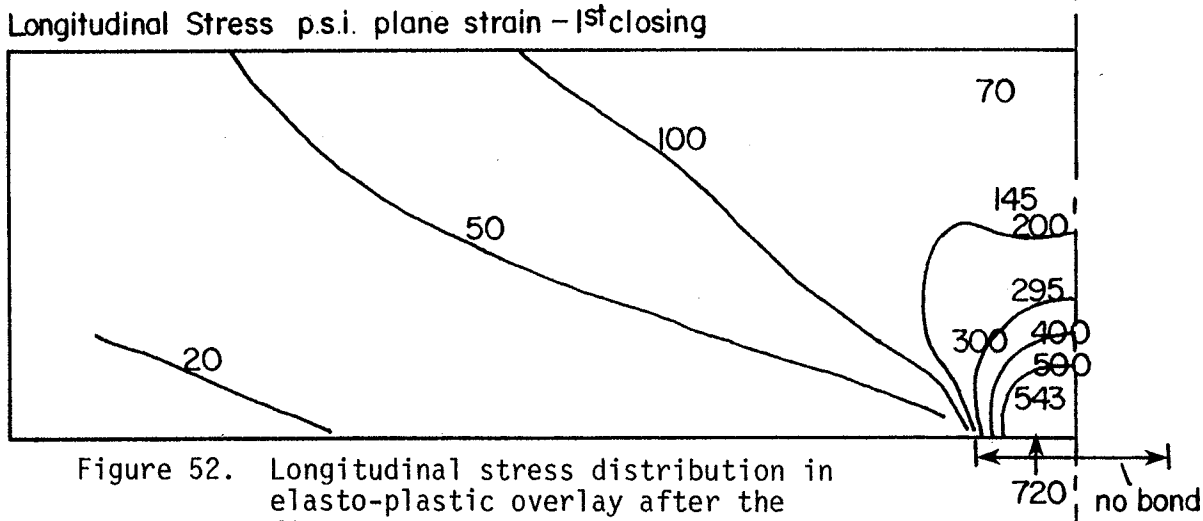

Figure 52. Longitudinal stress distribution in elasto-plastic overlay after the first crack reclosing.

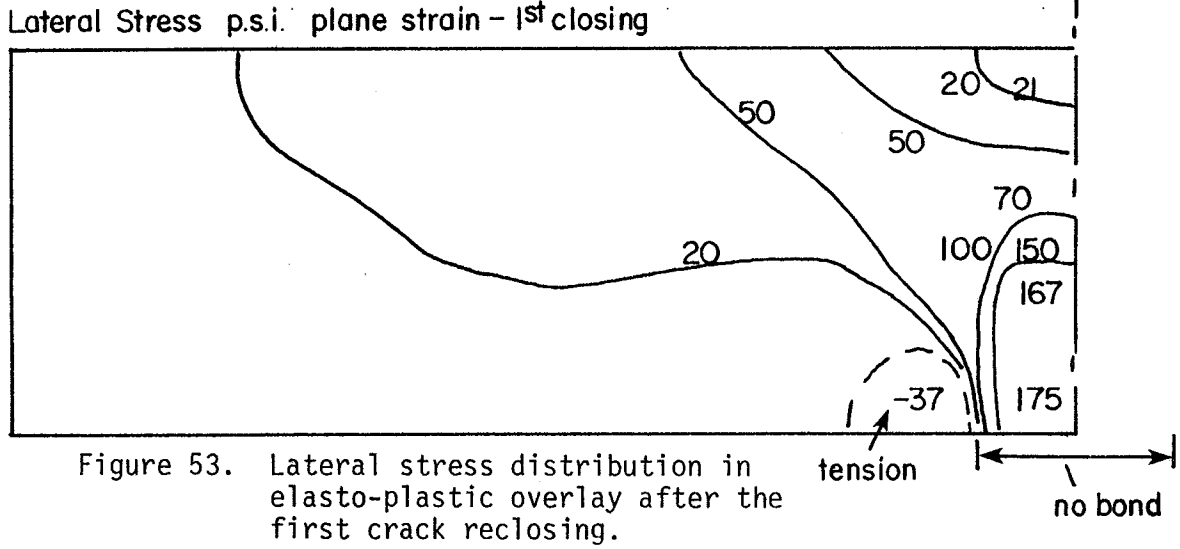

Figure 53. Lateral stress distribution in elasto-plastic overlay after the first crack reclosing.

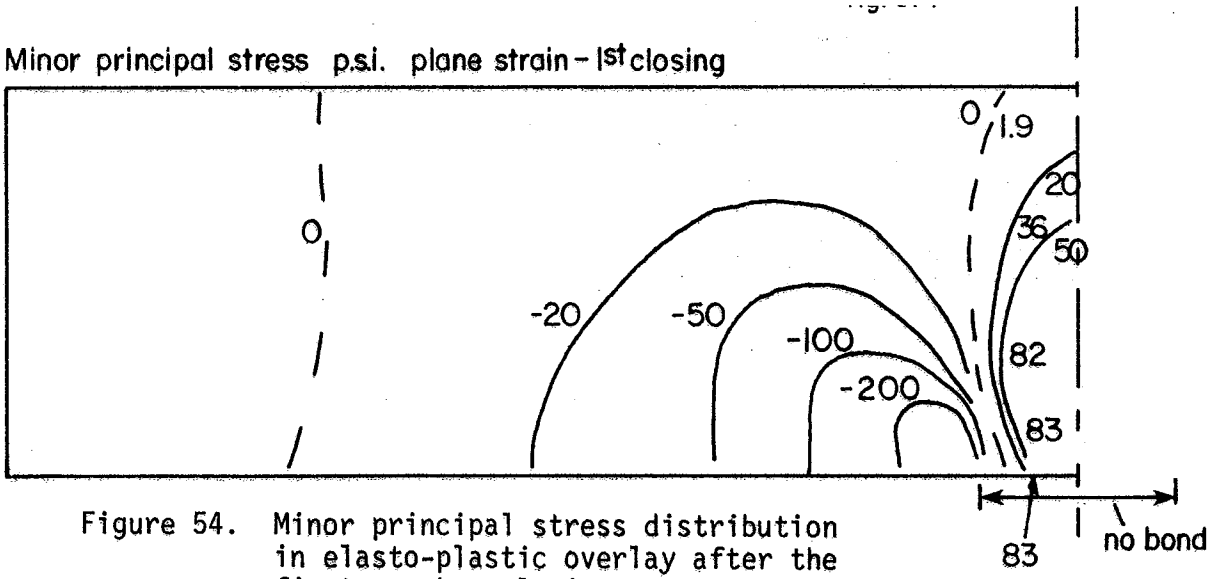

Figure 54. Minor principal stress distribution in elasto-plastic overlay after the first crack reclosing.

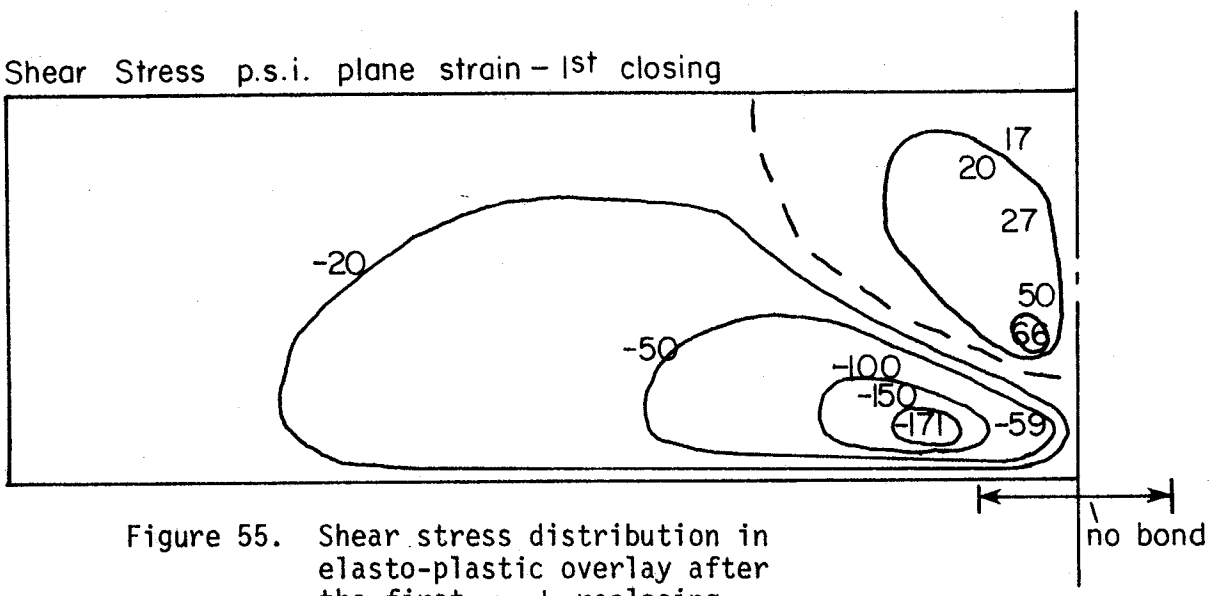

Figure 55. Shear stress distribution in elasto-plastic overlay after the first crack reclosing.

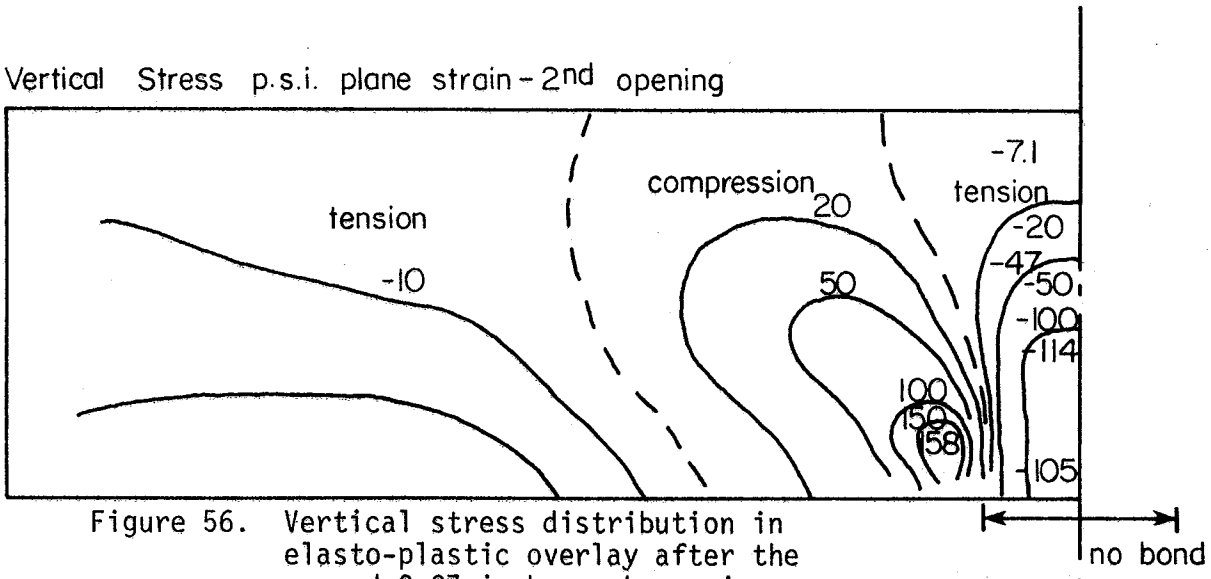

Figure 56. Vertical stress distribution in elasto-plastic overlay after the second 0.07 inch crack opening.

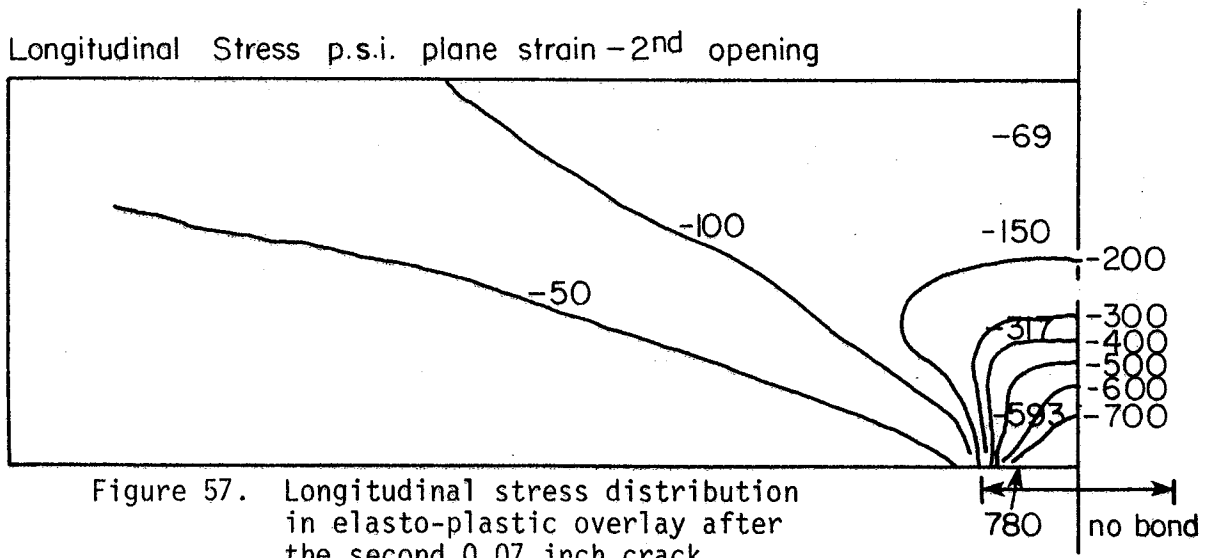

Figure 57. Longitudinal stress distribution in elasto-plastic overlay after the second 0.07 inch crack opening.

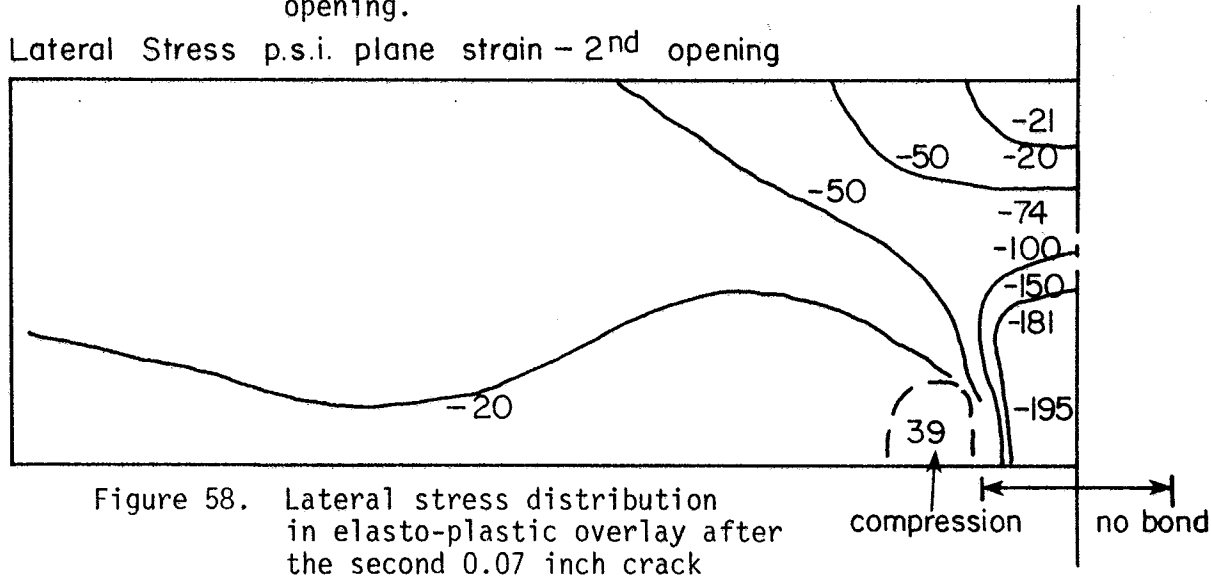

Figure 58. Lateral stress distribution in elasto-plastic overlay after the second 0.07 inch crack opening.

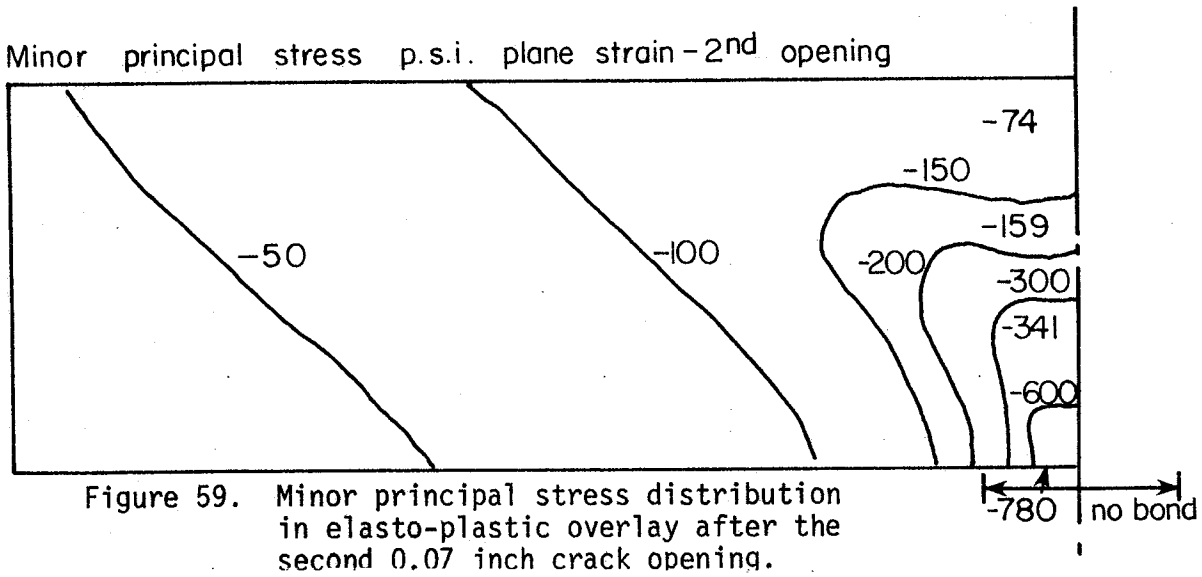

Figure 59. Minor principal stress distribution in elasto-plastic overlay after the second 0.07 inch crack opening.

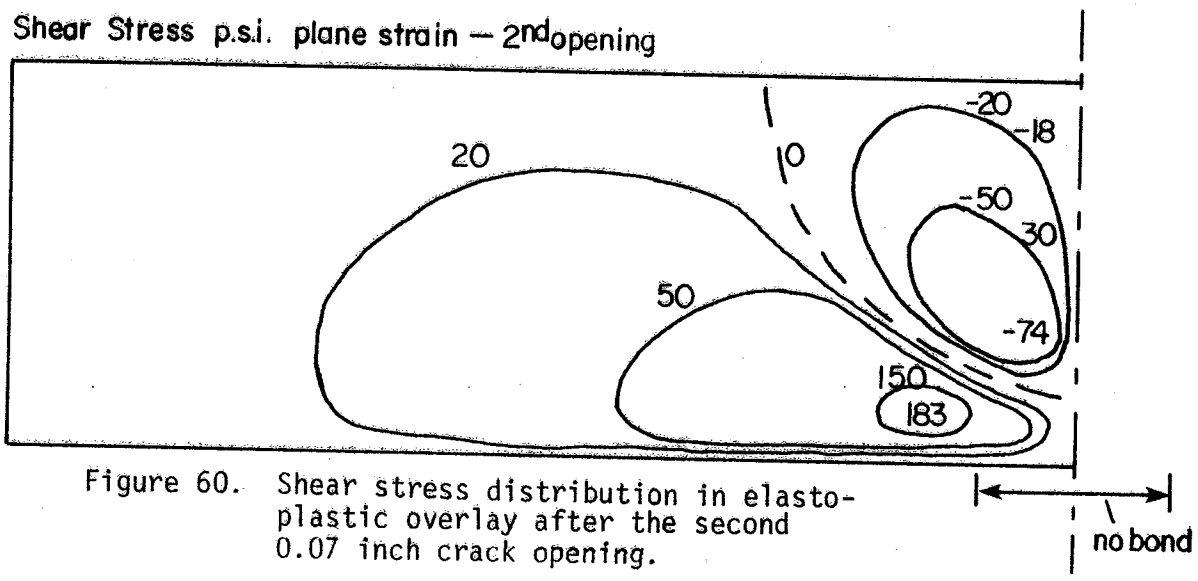

Figure 60. Shear stress distribution in elasto-plastic overlay after the second 0.07 inch crack opening.

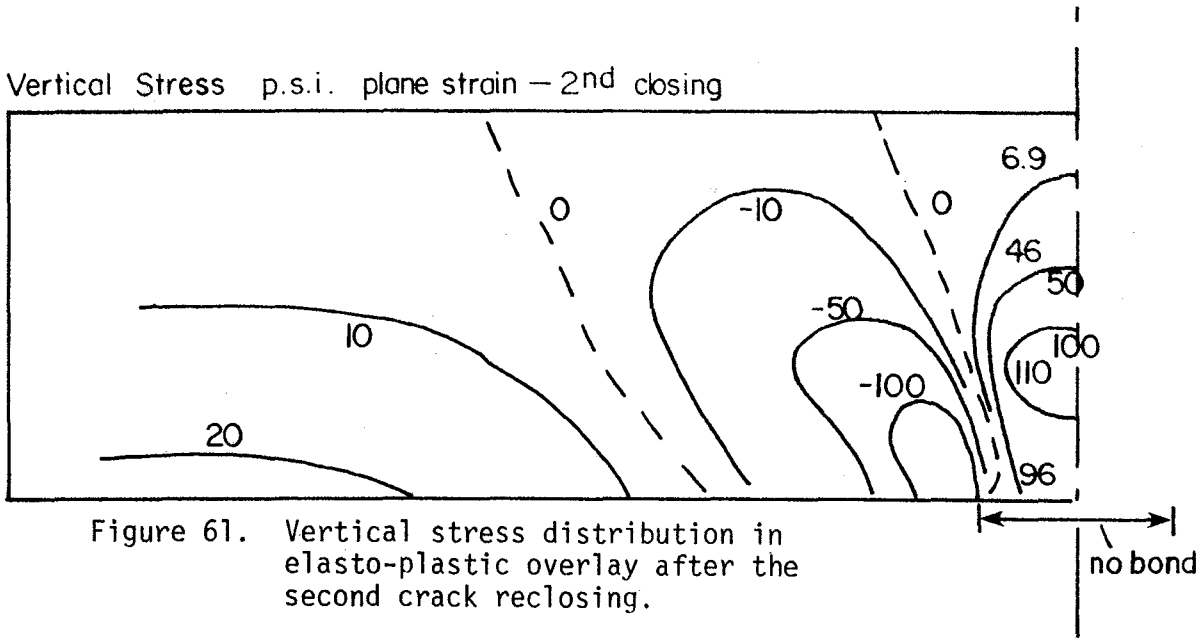

Figure 61. Vertical stress distribution in elasto-plastic overlay after the second crack reclosing.

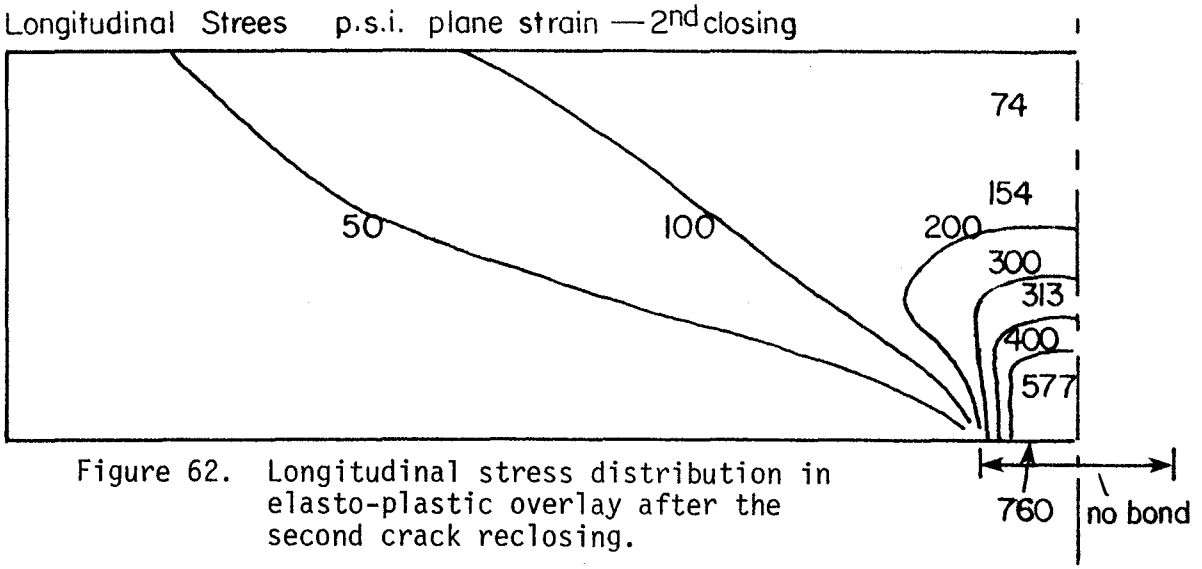

Figure 62. Longitudinal stress distribution in elasto-plastic overlay after the second crack reclosing.

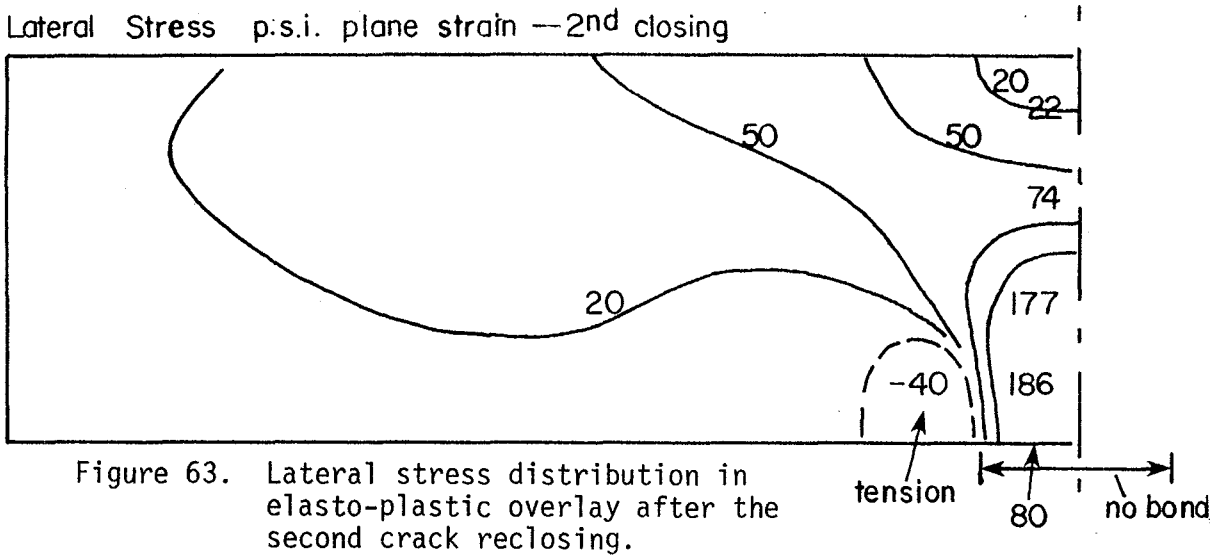

Figure 63. Lateral stress distribution in elasto-plastic overlay after the second crack reclosing.

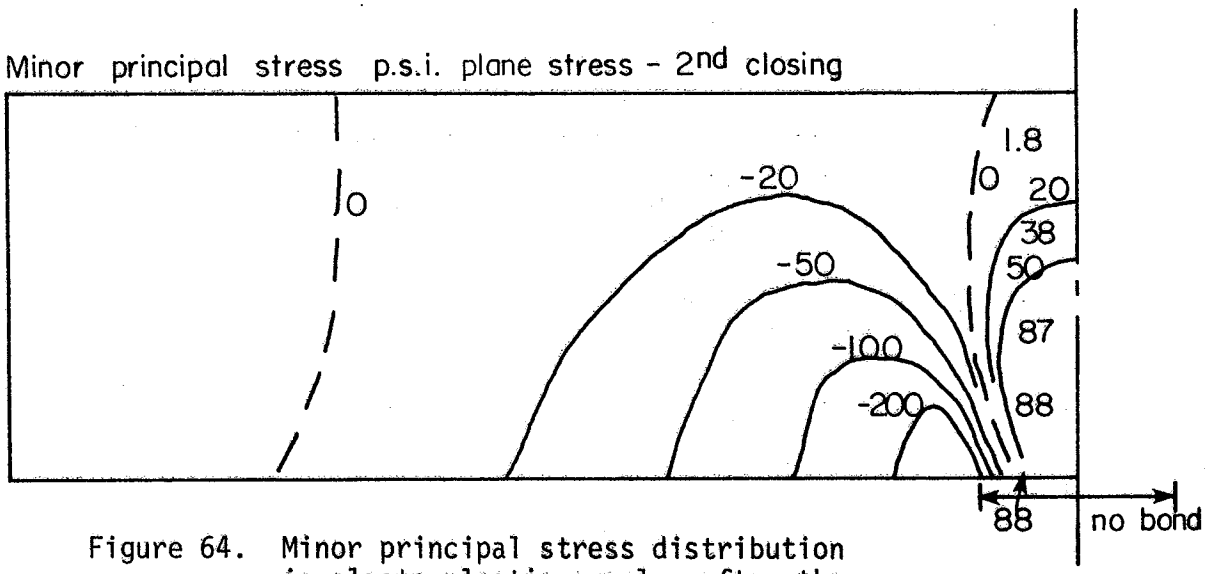

Figure 64. Minor principal stress distribution in elasto-plastic overlay after the second crack reclosing.

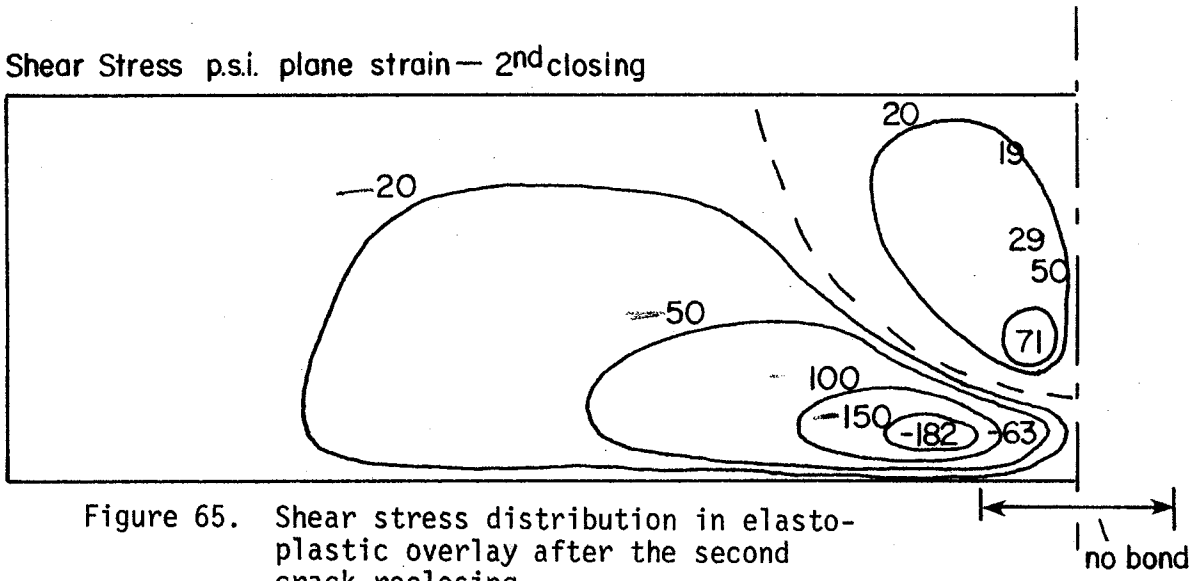

Figure 65. Shear stress distribution in elasto-plastic overlay after the second crack reclosing.

the maxumum compression will be about 850 p.s.i.

It is interesting to compare Figure 66, which relates peak longitudinal stresses near the underlying pavement crack to crack opening, with Figure 45 which relates total tensile or compressive load to crack opening in the laboratory study. The similarities are that the theoretical peak cyclic tensile stress decreases relative to the theoretical peak cyclic compressive stress, just as the peak tensile load decreases relative to the peak compressive load in the laboratory experiment. One difference between the two sets of behavior is that cracks appear in the laboratory overlay after three cycles. By the 100th cycle the compressive behavior remains approximately elasto-plastic but the tensile behavior becomes elastic-perfectly plastic. It seems likely that the perfectly plastic tensile part of the curve is due to that part of the crack which healed during compression progressively opening during tension. This non-symmetric phenomenon together with our newly acquired ability to calculate all stresses in and near the crack region provides a means of calculating the crack length from laboratory overlay tests rather than relying on visual observation.

It is of interest to note that the vertical stresses have two zones of tension and one of compression while the crack is being pulled open and one of tension and two of compression while the crack is being pushed closed.

The most extreme minor principal stresses (Figures 49, 54, 59, and 64) settle down to range between about 90 p.s.i. compression and 780 p.s.i. tension.

The lateral stresses (Figures 48, 53, 58, and 63) in the critical region, cycle between 195 p.s.i. tension when pulling and 180 p.s.i. compression when pushing. The plane strain condition causes the sum of

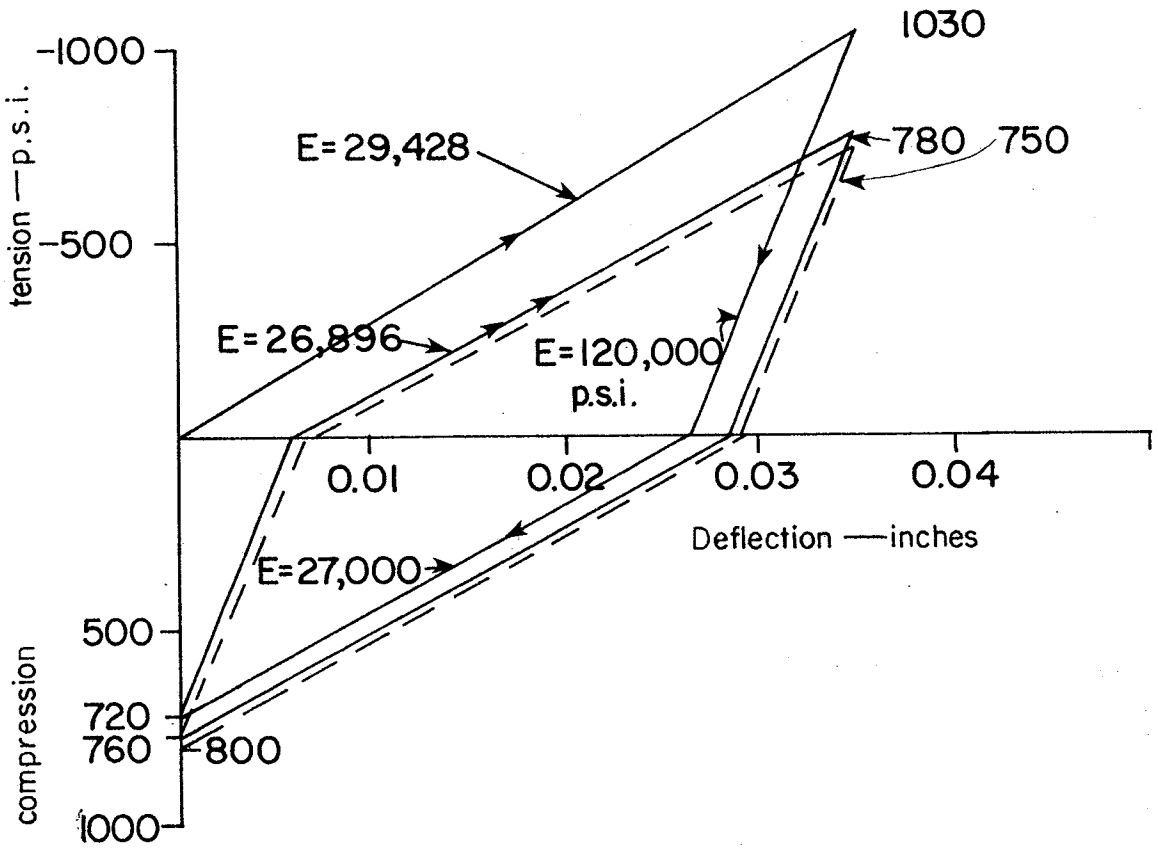

Figure 66. The calculated peak cyclic stresses verus crack opening; adjacent to opening and closing crack under simulated overlay.

principal stresses in the overlay crack region to reduce while the crack in the old pavement is opening. This weakens the overlay. But the compressive lateral stresses occurring when the crack is closing at a time when the overlay is hot may help in the healing process.

The shear stress peaks (Figures 50, 55, 60, and 65) occur near the interface of the underlying pavement next to the region of separation. It cycles between positive and negative and ranges from 224 p.s.i. at first pull to a steady cycling between $\pm$ 183 p.s.i. It is easy to see that further separation must occur when the length of separation is initially small. Reflection cracking would be reduced if the bond strength between the underlying pavement and the overlay was carefully limited so that separation would easily occur near the cracks and if sufficient overlay shear strength were provided to prevent shoving.

It may be of interest to note from shear stress plots that there is a common line of zero shear for opening and closing. That is, along this line the principal stresses are always parallel to the surface of the overlay.

Strains

It has been seen that reversing stresses settle down to fixed cycles after the first six crack openings and closings. By contrast there appears to be a continual horizontal movement of the overlay material towards the region above the opening and closing crack. This phenomenon is be observed by comparing Figures 67 and 68 with Figures 69 and 70. The material moves toward the crack after each pull and push. Material flows from the region farthest from the crack, reducing the overlay thickness

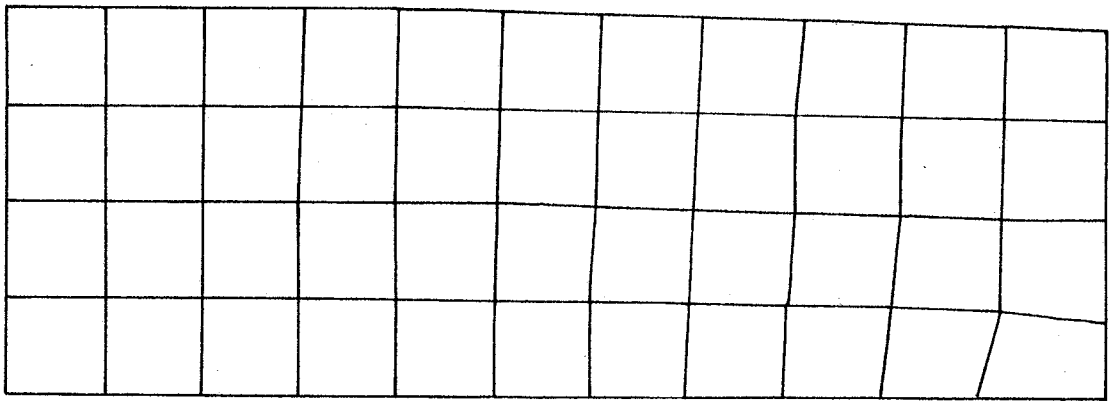

Figure 67. Longitudinal and vertical deflections after the first crack opening. Scale: 0.1" = 0.02" defl^{n}

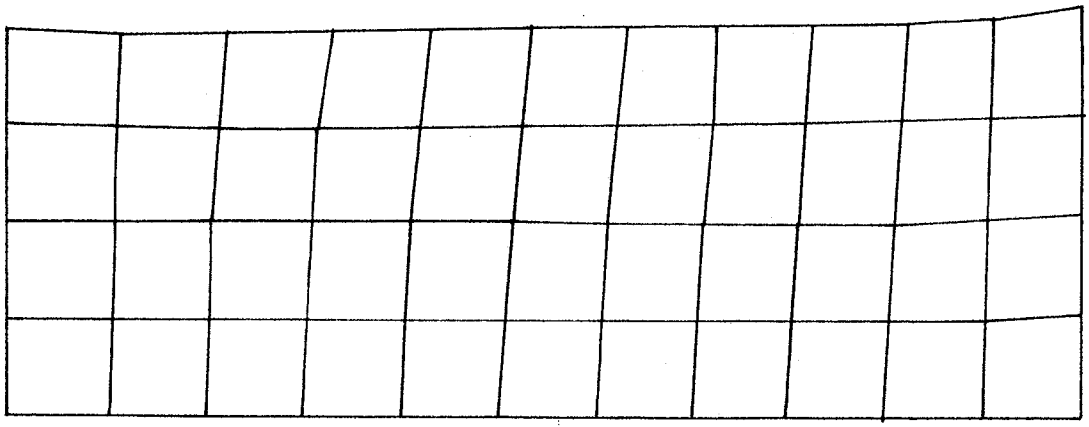

Figure 68. Longitudinal and vertical deflections after the first crack reclosing. Scale: 0.1" = 0.0004" defl^{n}

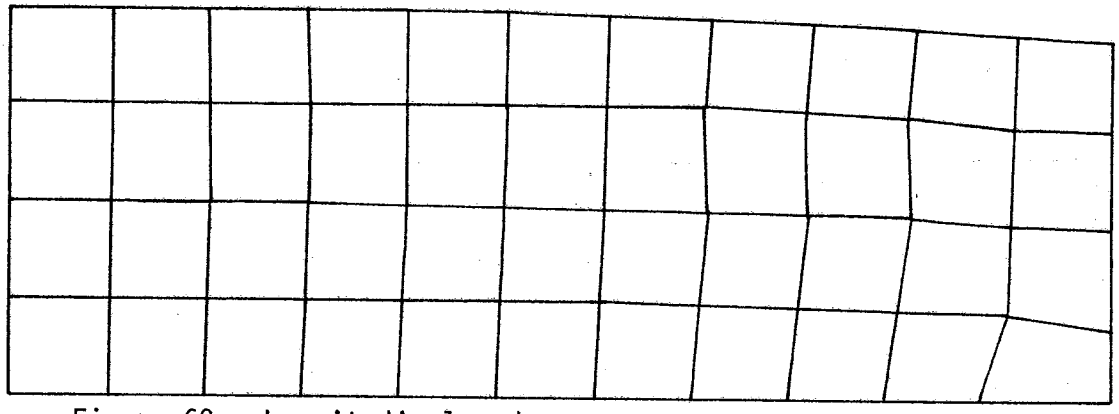

Figure 69. Longitudinal and vertical deflections after the second crack opening.

Scale : 0.1" = 0.02" defl

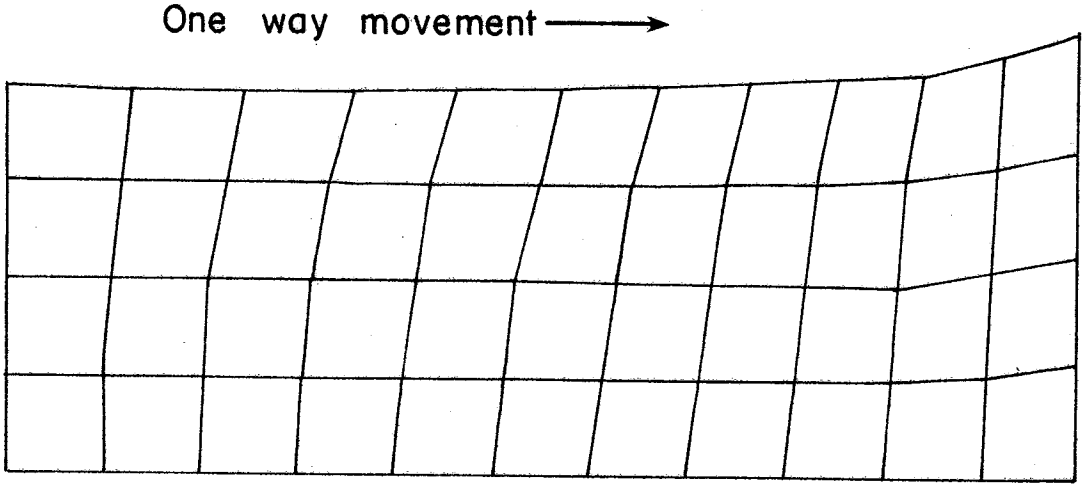

Figure 70. Longitudinal and vertical deflections after the second crack reclosing.

Scale : 0.1" = 0.0004" defl

there, to build up increasing thickness over the crack. Accordingly humps should form in overlays over sites of potential reflection cracking. The hump would be pounded by the traffic causing increased compaction and possibly help to heal any cracking in the overlay.

The Combined Effect of Repeated Rolling and Repeated Longitudinal Tension-Compression in Overlays

We have seen that for an asphaltic overlay material (loading modulus of 30,000 p.s.i.) the cyclic tension-compression of an underlying pavement crack opening and closing is between a tension of 700 p.s.i. and a compression of 850 p.s.i. If the material was of a similar rigidity to the one simulated in the repeated rolling analysis earlier in this report, this cyclic range would have been 115 p.s.i. tension to 141 p.s.i. compression.

With no change of material properties the wheel load with 50 p.s.i. contact stress would require 109 passes to build up the residual longitudinal stress of 115 p.s.i. compression and thus cancel the tension due to crack opening. Accordingly, no crack can form unless by another mechanism, provided that:

(i) The potential crack is transverse.

(ii) The materials are not changed by the cyclic stressing.

(iii) There is no other interaction between the two mechanisms-repeated traffic loading and crack opening.

(iv) There are at least 109 wheel passes across each part of the crack site.

Another mechanism for causing the crack to form is the relative vertical deflection of the material on each side of the underlying pavement

REFERENCES

1. Battiato, G., Ronca, G., and Verga, C., "Moving Loads on a Viscoelastic Double Layer Prediction of Recoverable and Permanent Deformation," Proc., 4th Int. Conf. Struct. Design of Asphalt Pavements, Vol. 1, p. 459, 1977.

2. Yandell, W. O., "Stress Distribution Associated with Rolling Resistance," Austrailian Road Research, Vol. 3, No. 1, March, 1967.

3. Yandell, W. O., "Rolling Resistance and Stress Distribution Associated Plastic Hysteresis," Joul Inst. of Engineers Austriala, paper 2370, (Oct., Nov. 1967)

4. Yandell, W. O., "The Measurement of the Surface Friction of Stones with Particular Regard to the Frictional Properties of Road Surfaces," Ph.D. Dissertation, University of N. S. W., 1970.

5. Yandell, W. O., "The Prediction of the Behavior of Elasto-Plastic Roads During Repeated Rolling Using the Mechano-Lattice Analogy and the Results of Cyclic Load Material Tests," Highway Research Record No. 374, Washington, 1971.

6. Yandell, W. O., "A New Theory of Hysteretic Sliding Friction," Wear, 17 Switzerland, April, 1971.

7. Yandell, W. O., and Holla, L., "Prediction of the Coefficient of Friction from Surface Texture Measurement," Proc., 7th Conf. A. R. R. B., Adelaide, 1974.

8. Yandell, W. O., and Gopalan, M. G., "The Relation Between the Surface Texture of Roads and the Friction and Abrasion of Tire Tread Rubber," Proc., 8th A. R. R. B. Conf. Perth, Australia, August, 1976.

9. Yandell, W. O., "The Effect of Repeated Loading on Road Making Material," Master of Engineering, Dissertation University of N. S. W., 1966.

10. Sharma, M. G., et. al, "Evaluation of Flexible Pavement Design Methodology Based Upon Field Observations at P. S. U. Test Track," Proc., 4th Int. Conf. Struct. Design of Asphalt Pavements, Vol. 1, 1977, p. 158.

11. Brown, S. F. and Bell, C. A., "The Validity of Design Procedures for Permanent Deformation of Asphalt Pavements, 1977, Vol. 1, p. 467.